THE EFFECT OF NANOFIBER SURFACE MODIFICATION ON OSTEOGENIC STEM CELL DIFFERENTIATION

by

Günnur Onak

B.Sc., Biomedical Engineering, Namık Kemal University, 2013

Submitted to the Institute of Biomedical Engineering
in partial fulfillment of the requirements
for the degree of
Master of Science
in
Biomedical Engineering

Boğaziçi University
2019

ACKNOWLEDGMENTS

I would like to thank my advisor Bora Garipcan for his support during my thesis. And I am extremely grateful to meet my co-advisor Ozan Karaman. I am deeply thankful to him, for all the time he invested to teach me how to research and write a scientific paper.

I would like to also thank to Aydın Akan, Utku Kürşat Ercan and Nermin Topaloğlu Avşar. I would also like to thank my lab colleagues Emine Afra Demirci, Ziyşan Buse Yaralı, Çağla Yıldırım, Elif Çukur, Yusuf Hakan Usta for their support and contributions during my thesis. I would also like to thank my colleagues Res. Asst. Metehan Atagür, Res. Asst. Eyyüp Yalçın and Spec. Saadet Güler for their support and contributions during my thesis.

I would like to specially thank to Asena Gülenay Tatar, Caner Dikyol, Hatice Kübra Bilgili, Nursu Erdoğan and Zülal Muganlı. I consider myself lucky to meet them. I strongly believe that their dreams will come true soon.

I would also like to thank my close friends Doğan Onur Arısoy, Çağla Özsoy, Çiğdem Özkolaçık, İlayda Duru and Alican Onur Çankaya. I never forget the times in BOUN BME with them.

I would also like to thank my close friends in Katip Çelebi University İnci Develioğlu and Ömer Bilginer. They make my life in Izmir more enjoyable.

Finaly, I am grateful to have such a dedicated family who encouraged and supported me through all my life.

ACADEMIC ETHICS AND INTEGRITY STATEMENT

I, Günnur Onak, hereby certify that I am aware of the Academic Ethics and Integrity Policy issued by the Council of Higher Education (YÖK) and I fully acknowledge all the consequences due to its violation by plagiarism or any other way.

Name :

Signature:

Date:

ABSTRACT

THE EFFECT OF NANOFIBER SURFACE MODIFICATION ON OSTEOGENIC STEM CELL DIFFERENTIATION

Optimization of nanofiber (NF) surface properties is critical to achieve an adequate cell response. Here, the impact of conjugation of biomimetic aspartic (ASP) and glutamic acid (GLU) templated peptides with PLGA electrospun NF on osteogenic differentiation of bone marrow stromal cells (BMSCs) was evaluated. Cold atmospheric plasma (CAP) was used to functionalize the NF surface and thus to mediate the conjugation. The influence of the CAP treatment following with peptide conjugation to the NF surface was assessed using scanning electron microscopy (SEM), contact angle measurements, Fourier-transform infrared spectroscopy (FTIR) and X-ray photoelectron spectroscopy (XPS), Both the hydrophilicity of NFs and the number of the -COOH groups on the surface increased with respect to the duration of CAP treatment. Results demonstrated that CAP treatment significantly enhanced peptide conjugation on surface of NF. Osteogenic differentiation results indicated that conjugating of biomimetic ASP templated peptides sharply increased alkaline phosphatase (ALP) activity, calcium content, and expression of key osteogenic markers of collagen type I, osteocalcin, and osteopontin compare to GLU conjugated and neat NF. It was further depicted that ASP sequences are the major fragments that influence mineralization and osteogenic differentiation in non-collagenous proteins of bone extracellular matrix.

Keywords: Bone tissue engineering, Peptide, Scaffold, Surface functionalization.

ÖZET

NANOFİBER YÜZEY MODİFİKASYONUN OSTEOJENİK KÖK HÜCRELERİN FARKLILAŞMASI ÜZERİNE ETKİSİ

Nanofiber (NF) yüzey özelliklerinin optimizasyonu, yeterli hücre yanıtı elde etmek için kritik öneme sahiptir. Bu çalışmada, biyomimetik aspartik (ASP) ve glutamik asit (GLU) peptidlerinin PLGA elektrospun NF üzerine konjügasyonunun, kemik iliği mezankimal kök hücrelerinin (MKH) osteojenik farklılaşması üzerinde etkisi değerlendirilmiş ve NF yüzeyini fonksiyonel hale getirmek ve böylece konjügasyona aracılık etmek için soğuk atmosferik plazma (SAP) kullanılmıştır. Peptit konjügasyonu için kullanılan SAP muamelesinin NF yüzeyine etkisi, taramalı elektron mikroskobu (SEM), temas açısı ölçümleri, Fourier-dönüşümlü kızılötesi spektroskopi (FTIR) ve X-ışını fotoelektron spektroskopisi (XPS) kullanılarak değerlendirilmiş ve muamele sonucu yüzeydeki -COOH gruplarının sayısının attığı saptanmıştır. Sonuçlar, SAP muamelesinin, NF'in yüzeyinde peptit konjügasyonunu önemli ölçüde artırdığını göstermiştir. Osteojenik farklılarşma sonuçları, biyomimetik ASP peptidlerin konjügasyonunun , alkalin fosfataz (ALP) aktivitesini, kalsiyum miktarını ve önemli osteojenik markörler olan kollajen tip I, osteokalsin ve osteopontinin ekspresyonunu, GLU konjüge edilen NF ve NF'e kıyasla arttırdığını göstermirştir. Ayrıca, ASP dizilerinin, kemik dışı hücre dışı matrisin kolajen olmayan proteinlerinde minerallerşmeyi ve osteojenik farklılaşmayı etkileyen başlıca fragmanlardan olduğu ileri sürülmüştür.

Anahtar Sözcükler: Kemik Doku Mühendisliği, Peptit, Doku İskelesi, Yüzey Fonksiyonelleştirme.

TABLE OF CONTENTS

LIST OF FIGURES

LIST OF TABLES

LIST OF SYMBOLS

θ	contact angle

LIST OF ABBREVIATIONS

3-D	3- dimensional
MSCs	Mesenchymal stem cells
ECM	Extracellular Matrix
HA	Hydroxyapatite
DEX	Dexamethasone
OP	Osteopontin
ON	Osteonectin
OC	Osteocalcin
BSP	Bone Sialoprotein
PCL	Polycaprolactone
PLG	Poly(lactide-co-glycolid
PLA	Poly (L-lactic acid)
PLGA	poly (lactic-co-glycolic acid)
FDA	Food and Drug Administration
SEM	Scanning Electron Microscopy
XPS	X-ray Photoelectron Spectroscopy
MBHA	4-Methylbenzhydrylamine
Fmoc	9-fluorenylmethoxycarbonyl
HOBt	hydroxybenzotriazole
DMF	N-Dimethylformamide
FITC	Fluorescein isoth-iocyanate
DCM	Dichloromethane
DIEA	N, N-diisopropylethylamine
MES	2-Morpholinoethanesulfonic acid buffer
pNPP	p-nitrophenylphosphate
GAPDH	glyceraldehyde 3-phosphate dehydrogenase
DAPI	4,6-diamidino- 2-phenylindole

1. INTRODUCTION

1.1 Motivation

Allogeneic and autologous bone grafting are considered as the treatment standarts to manage bone diseases such as bone defects and cranial, maxillofacial, oral fractures [1, 2]. By 2017, more than 2 million bone grafts are required by number of injuries including traffic accidents, wars or tumor removal, worldwide each year [3]. Several limitations in the clinic including immune response, donor-site morbidity, long recovery times, loss of mechanical and biologic properties and lack of availability are experienced in these procedures [4, 5]. Some alternatives have been explored to current treatment strategies to overcome the difficulties. Tissue engineering as an alternative to current strategies is based on the principle of maintaining 3-D (3- dimensional) substrate for cells to function and replacing damaged tissues with cell supporting scaffolds.

In terms of applicability of bone tissue engineering strategy, the aim is to initiate healing response of bone tissue in a precise anatomic area. Therefore, the regenerated tissue should be integrated with the surrounding tissue. Biomechanical properties of formed tissue should be durable and effective [6]. Numbers of biological and mechanical factors affect ordered cellular events to repair and regenerate the bone in the tissue engineering process. First, tissue formation necessitates the presence of bone forming cells which is called osteoprogenitor cells. Once an appropriate number of osteoprogenitor cells have been harvested from many sites of the body to provide the required population, they should be delivered into the skeletal defects to initiate the bone healing process and integrate with the surrounding tissues. Naturally or synthetic scaffolds which act as passive 3-D structured matrices, support this process by enhancing cell attachment, proliferation, and differentiation. They enhance the bone healing response to progress throughout the defects by helping the cells to create their own matrix and integrate with the host tissue as the implant degrade by the time [7].

1.2 Aims

The aim of this thesis is to produce MSCs(mesenchymal stem cells) seeded bone mimetic scaffolds to be used as a suitable synthetic matrix in bone tissue engineering studies to regenerate bone defects. Scaffolds used in bone tissue engineering are required to have specific features such as easy to implant, appropriate physical and mechanical properties, biodegradable, osteoconductive, biocompatible and cost effective. Due to the reason that tissue engineered scaffolds will be used to treat the complex bone defects, these scaffolds should have similar functional and structural properties of bone tissue. The potential of peptide-templated bone mimetic scaffolds for bone regeneration showed in this thesis will be useful for clinical development.

1.3 Outline

In the first part of this thesis (Background), a description of the anatomy and physiology of the bone are given. The first part is followed by bone tissue engineering and biomaterials for scaffold fabrication. Then, fabrication techniques and functionalization techniques of biomimetic scaffolds were covered, respectively. In the second part, the methods used to produce biomimetic scaffold for bone tissue were given. First, the methodology for characterization of peptide-nanofiber conjugation is given. Second, analysis for osteogenic differentiation of hMSCS on nanofibers are covered. In the last part, results are explained and discussed. To conclude the thesis, planned future work on biomimetic scaffold fabrication is discussed.

2. BACKGROUND

2.1 Biology of Bone Tissue

2.1.1 Bone Tissue

Tissue is a group of cells that perform similar functions in the body. More than 200 different cell types in human body are organized into four main tissues: epithelial, connective, nervous and muscle tissues. Bone tissue is a dense connective tissue, which has extracellular matrix (ECM) in addition to the cells. Most connective tissues have nerves and blood supply and consist of scattered cells submerged in the ECM. The characteristics of the matrix can be identified by structural networks and intracellular materials consists of different amount of fibers and ground substances. The bone tissue consists of organic composite fibrous protein and collagen network (30-35% of the weight) covered with a stiff matrix of inorganic calcium/phosphate (65-70% of the weight) [8]. While the organic materials and mineral salts creates its major characteristic function by giving the matrix compression strength, collagen provide the flexibility and resistance [9] - [12].

Mesenchymal stem cells (MSCs), which connective tissue originates from, have ability to differentiate into specific cell lines. Osteoprogenitor cells as basic stem cells of bone structure have ability to differentiate chondroblasts or osteoblasts. If osteoprogenitor cells are positioned close to oxygen rich locations such as capillaries, they differentiate into osteoblasts; otherwise they become chondroblasts due to low oxygen concentration levels. Bone cells can be categorized in four parts which have all different functions and origins: osteoblasts, osteocytes, osteoclasts, and osteoprogenitors. Osteoblasts are highly secretory bone cells that derived from osteoprogenitor cells. They form bone by producing collagen and proteoglycans with their large endoplasmic reticulum and numerous ribosomes. The secretory products of osteoblasts are noncollagenous proteins including osteopontin, osteocalcin, and bone sialoprotein and

in particular type 1 collagen. The formation of bones by osteoblasts is called ossification or osteogenesis. The bone extracellular matrix (ECM) which surrounds the cells are formed by the interaction between osteoblasts. Osteocytes are mature osteoblasts which are formed after an osteoblast starts to be surrounded by bone ECM. Small cavities in the bone which are called lacunae are occupied by osteocytes. The osteocytes do not secrete bone matrix. The osteocytes conform the shapes of matrix surrounding them. They respond to stress and strain such as bone deformation and bone loading and send signals to osteoblast and osteoclasts to build up or degrade the bone matrix. Osteoclasts are the only cells in nature that can degrade mineralized bone tissue by producing related enzymes. This function is crucial for bone growth, modeling and remodeling [9] - [12].

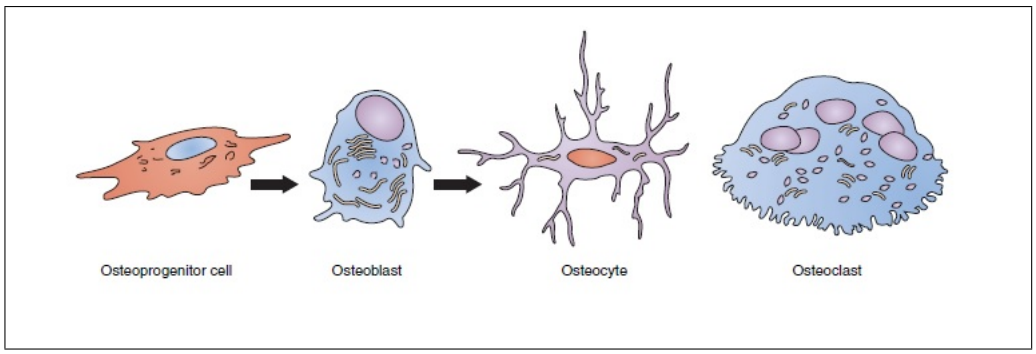

Figure 2.1 The different types of bone cells [11].

2.1.2 Bone Structure and Functions

Bone is a living and continuously changing tissue. The composition and structure of cortical and cancellous bone support the skeleton to mechanically function. Since the cortical bone is relatively stiff compared to cancellous bone, it responds more slowly when the load is changed. The cancellous bone has a high surface to volume ratio and high metabolic activity. Cortical bone consists of cylindrical structures called osteons. An osteon, also called Haversian canal, provides effective metabolism for bone cells enclosed by concentric rings of mineral salts. This central canal is surrounded by blood vessels (capillaries, arterioles, venules) and nerves. The matrix and osteocytes are laid down in rings of bone. Each layer of the rings is called lamella. Several small

cavities called lacunae are positioned between two lamellae or rings of bone. Each lacuna consists of an osteocyte in tissue fluid. Blood vessels and the osteocytes exchange oxygen, nutrients and waste products. The blood vessels in the periosteum are connected to these blood vessels which perforate the central canals are connected. The periosteum covers the bone by passing through Volkmann's canals. Volkmann's canals run through horizontally to the Haversian (central) canals. Cortical bone tissues are positioned at the outside surface of other bones. Cancellous bone, which forms the center of all other type of bones, is positioned at the ends of long bones. It consists of an irregular latticework called trabeculae. The trabeculae which is interconnecting sections of bone, creates the sponge-like structure of cancellous bone. Bone vessels and bone marrow fills the spaces between the trabeculae. Blood vessels in the marrow transfer nutrients by diffusion through the canaliculi of the lamellae to the osteocytes in the lacunae. These blood vessels have connection with the blood vessels in the Volkmann's and Haversian canals. In contrast to cortical bone, cancellous bone has no osteons. Cancellous bone is found inner part of the bones, cortical bones are positioned on the surface of a bone for protection. Bones are supporting structure which have the attachment of muscles and other tissues. Bones protect vital organs in the body such as the skull protecting brain, the ribs protecting the lungs and heart. Tissue stabilization around the bone, such as muscles, skin, nerves, blood and fat, are also provided by the bone. Bones produce blood cells. This process is called hematopoiesis and occurs essentially in red bone marrow in the medullar cavity of long bones. Essential minerals, especially phosphorus and calcium, and fats are stored [10, 11, 13].

2.1.3 Bone Types

Bones may be classified according to their various properties, such as shape, origin, and texture. There are five types of bones in the human body: long, short, flat, irregular, sesamoid, and sutural bones. Long bones are bones whose length exceeds their width such as limbs, fingers and toes. Long bones contain a diaphysis (shaft), a metaphysis (flared) and two extended ends, each called an epiphysis. While the metaphysis is made of cancellous bone, the diaphysis is composed mainly of compact

tissue called shaft. The interior of the shaft is surrounding a central cavity which is called medullar cavity. Yellow bone marrow located in the medullar cavity. Epiphysis consists of cancellous bone which usually contains red marrow and have a thin layer of compact tissue. The outer layer of epiphysis is attached by hyaline cartilage. The outside of the long bone is covered by the periosteum. Short bones have merely similar structure to long bones. They lack a long axis such as the tarsal bones of the foot and the carpal bone of the wrist. Flat bones, which are thin and usually curved bones, provide surface area for muscle attachment and protection for vital soft parts of the body. Flat bones are composed two flat plates of compact bone tissue enclosed by a layer of cancellous bone. Examples of flat bones are the roof of the skull, the sternum, scapula, ribs, and, parts of the pelvic bones. Irregular bones have peculiar and complex shapes. Irregular bones are also composed of cancellous bone surrounding with compact bone in thin layers. They are located at the ossicles of the ears and the vertebrae. Sesamoid bones are small, flat, and rounded bones. Sesamoid bones which located adjacent to joints, surrounded with tendon and fascial tissue. Some of the sesamoid bones are the bones of kneecap, patella, the wrist and ankle [10, 11, 13].

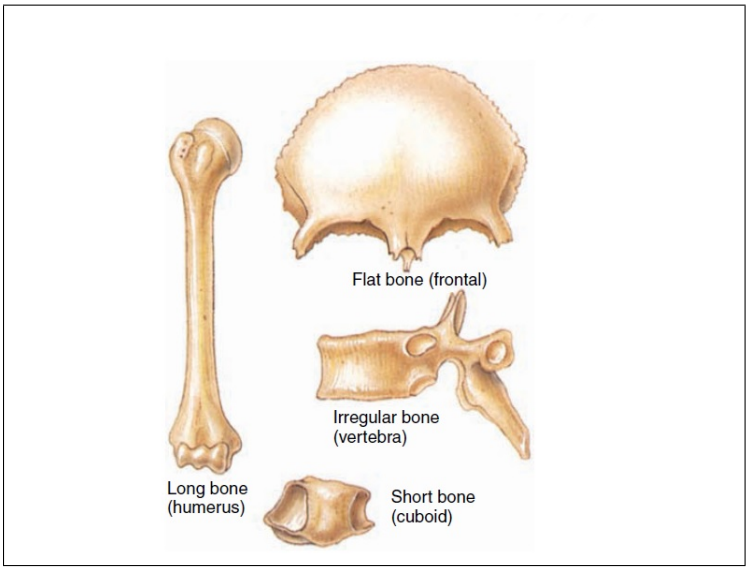

Figure 2.2 The classification of bones based on shape [11].

2.1.4 Bone Development and Growth

The formation of skeleton in fetus continues until the end of the third month of pregnancy. At this time, the skeleton mostly consists of cartilage. In the following months of pregnancy, ossification is followed by bone formation and growth. The ossification process initiates with invasion of the osteoblast to the cartilage. Bone growth in longitudinal direction which takes place at the epiphyseal line, continues until the age of 15 in girls and the age of 16 in boys. Bone maturation and remodeling process finishes at the age of 21. Cartilage provides environment for the bone development from mesenchymal cells during these critical processes. Bone elasticity under applied tension is provided by strong protein matrix whereas bone strength under a pressure is enabled by the mineral salts deposited into this protein matrix. Bone is formed under the periosteum from spindle-shaped cells osteoblasts by differentiating to osteoprogenitor cells which are called undifferentiated bone cells. The osteoblasts are also located in the bone marrow and medullary cavity called endosteum. When the amount of strain or pressure increases, calcification, which is called the deposition of by the calcium salts, occurs. Osteocytes proliferation and secretion of matrix is stimulated by a break in the bone to form new bone. Furthermore, osteoclasts located in bone cavities remove bone from inner side and provide reabsorption during remodeling. Osteocytes (mature osteoblasts) deposit the new bone, while the old bone is removed by the osteoclasts remove the old bone. This remodeling process provides properly to heal the bone [13, 10, 11].

Ossification is the process refers tissue replacement to bone tissue. The types of ossification are intramembranous and endochondral ossification. In intramembranous ossification, the main source of bone tissue are mesenchymal cells and fibrous connective tissue. It starts with the differentiation of osteoblasts in fibrous connective tissue and takes place in the deeper layers of the dermis. The membrane of connective tissue with oriented fibers are formed by embryonic mesenchyme followed by differentiation of osteoprogenitor cells to osteoblasts to produce bone matrix to around the aligned collagen fibers. Larger trabeculae are produced by the rest of osteoblasts collected in the surface of the trabeculae to develop cancellous bone. Red bone marrow which is lo-

cated in the inner part of cancellous bone, was developed by the cells . The periosteum is created by the cells located in the outer part of the bone following the cancellous bone formation. The outer surface of the cortical bone is formed after developing the periosteum and bone matrix by osteoblasts. In endochondral ossification process, existing cartilage initiates bone differentiation. After four week in development process, the formation of hyaline cartilage is developed by chondroplasts differentiated from the mesenchymal cell. Chondrocytes are formed after chondroplasts are covered with cartilage matrix and surrounded with perichondrium. Osteoprogenitor cells are produced from osteoblasts after blood vessels are connected to perichondrium. Osteoblasts keep producing bones and perichondrium becomes periosteum to produce the bone structure [10, 11, 13].

2.2 Bone Tissue Engineering

Tissue engineering is an approach which combines the principles of biology and engineering by using different scientific fields in order to mimic human tissues. Bone tissue engineering is also interdisciplinary research area which offers alternatives to allografts and autografts by using synthetic grafts to support tissue regeneration [14, 15]. Bone tissue engineering deals with fabricating 3 dimentional scaffolds which resemble the extracellular matrix, support mechanically and provide formation of bone tissue. Scaffolds should perform osteo-inductive, osteo-conductive and osteogenic characteristics to enhance cell adhesion, proliferation,and spreading of cells. Furthermore, these scaffolds can be produce to enable biological and chemical factors which facilitate osteoblastic lineage [16] - [18]. Scaffolds with suitable structure induce cell attachment, proliferation and differentiation. Also, scaffolds should degrade after the formation of new bone tissues by facilitating complete replacement of cells and growth factors. Bone tissue engineering comprise of biomaterials, cells and appropriate surface properties of bone grafts for mineralization and regeneration of damaged bone tissue [19]. There are variety of biomaterials being used for bone tissue engineering studies such as ceramics, composites, and polymers [20]. Moreover, the techniques are available for scaffold preparation to gain characteristics such as the high surface to volume ratio, durability,

and morphological similarity to ECM [19]. Surface modification techniques have been studied for optimal bone tissue regeneration. Surfaces of scaffolds can be modified to improve the chemical and physical properties without losing integrity [20].

2.3 Biomaterials for Bone Tissue Engineering

Natural and synthetic materials have been manufactured for providing biomimetic scaffold and extracellular-matrix environments and for regeneration of bone tissue [21]. Scaffolds composed of natural or synthetic materials with tunable properties that can successfully mimic natural tissue are one of the major targets in tissue engineering. Synthetic and natural materials are being generally integrated in 3-D scaffolds for control of cell behaviour. Biological recognition that positively supports cell adhesion and function can be considered as one of the advantages of naturally derived materials. Nevertheless, they have disadvantages such as less control over their mechanical properties and biodegradability. Even though, unmodified synthetic materials have been prefered to used in applications of tissue engineering , they have a disadvantage which is lack of bioactive cues on their surface to support cell-matrix interactions for attachment, spreading, and differentiation. In this part, generally used polymers in bone tissue engineering are focused.

Natural polymers, which used in the very first biodegradable scaffolds in applications of bone tissue engineering, are generally derived from carbohydrates or proteins [22]. Natural polymers have variety of advantages such as biocompatibility and biodegradability. Nevertheless, these polymers require some modifications due to risk of triggering immunological response and inadequate mechanical strength after implantation. Here, most widely used natural polymers; collagens, chitosan and gelatin, for fibrous structure fabrication in bone tissue engineering studies are covered . The major protein in bone ECM is collagen which is considered as an ultimate material for scaffolds in tissue engineering [23]. Collagen type I is one of the popular collagen type, since bone ECM is rich in collagen type I [24]. Collagen supports several connective tissue types such as bones, tendons, cartilage, skin, ligaments, and blood vessels,

and provides crucial signals to regulate cell proliferation, migration, and differentiation [25, 26]. High mechanical strength for in vivo studies of the scaffolds for bone regeneration is critical. Therefore, collagen scaffolds for bone tissue engineering should be hardened with mineralization and by combining with hydroxyapatite crystals. Recently, many collagen-originated scaffolds have been studied in bone tissue engineering. Ying *et al*. loaded dexamethasone (DEX) to biphasic calcium phosphate nanoparticles and prepared collagen porous composite scaffolds [27]. While the composite scaffolds had high mechanical strength and interconnected pore structures, they also had a continuous release of DEX. Furthermore, this composite scaffolds were biocompatible and enhanced osteogenic differentiation of hMSCs. Chitosan, which is produced from chitin, is another essential natural polymer. Several forms such as fibers and films can be produced by modifying chitosan. Nevertheless, chitosan-based scaffold cannot load bearing bone grafts. To promote mechanical strength and structural integrity of chitosan, metals, ceramics and other polymers are combined with chitosan, and can be used as hydrogels, films and electrospun fibers. In recent studies, the mechanical strength of chitosan biocomposites polymers have been increased by using polymers such as Polycaprolactone (PCL), gelatin, alginate, and nano ceramics such as SiO_2, TiO_2, HAp, ZrO_2 [28] - [30]. Gelatin is a natural polymer which is derived from collagen by hydrolysis and improves cell adhesion due to the RGD (arginine, glycine, and aspartate) binding sequence in its structure.

The advantages of synthetic polymers compared to natural polymers are relative lack of immunological response,reproducibility, and tunable properties such as mechanical strength and degradation ratio. Synthetic polymeric scaffold with adaptive biological, degradation and mechanical properties have gained attention for bone tissue engineering applications. The most attractive synthetic polymers in this field are Poly (L-lactic acid), Poly(lactide-co-glycolide) (PLG) and Polycaprolactone (PCL). These synthetic materials have good mechanical and biocompability properties and are approved by Food and Drug Administration (FDA). Various properties including strength, hardness, porosity, osteoconductivity and fabrication capability should be taken into consideration to design a scaffold in bone tissue engineering. The absence of biological cues on synthetic polymeric scaffold arises the need of further surface modifi-

cation. Most of the synthetic polymeric scaffold do not have required surface chemistry to conjugate functional proteins or peptides due to high hydrophobicity. Improved hydrophilicity along with the introduction of particular functional groups on the surface of scaffold plays an important role in adhesion, proliferation and spreading of cells.

2.4 Fabrication Techniques of Biomimetic Fibrous Scaffolds

It is critical that scaffolding materials can positively interact with surrounding tissue enhance the natural regeneration of stem cells [31]. Significant efforts have been undertaken to develop such for scaffolds used in regenerative medicine applications. Considering the usage of these engineered scaffolds in the body, biomimetic scaffolds must be designed they should have some characteristics such as possession of appropriate surface properties for improving stem cell attachement, spreading, and differentiation, low toxicity and immunogenicity, high porosity, and degradability that is adequate for specific tissues, with interconnection between pores to provide cell growth and nutrient and waste transport [32]. Biomimetic scaffolds must be designed to enhance the cell spreading and direct the cell to grow into 3-D space by mimicking the three-dimensional structure of natural bone tissue. The diameters of collagen fibers in natural bone tissue structured as fibrous network with diameter ranging from 50 to 500 nm [4]. The ideal fabrication techniques for biomimetic scaffold production should allow produce the nanofibrous structure of collagen nanofibers in natural bone. Some fabrication methods have been used to produce nanofibers, such as self-assembly [33], phase separation [34], and electrospinning [35].

Phase separation is used as a simple fabrication technique to produce nanofibrous scaffolds [36]. The phase separation process relays on solving the polymer in a solvent. The fiber network formation affected from some parameters such as polymer and solvent type, the temperature, and polymer solution concentration. The fiber diameter of ranging from 50-500 nm, scaffold porosity of 98% and small pore space between nanofibers can be obtained cells to migrate. Other fabrication techniques,such as particulate leaching,can be combined with phase separation to produce biomimetic

scaffolds with ideal pore size [37].

Self-assembly is a spontaneous self-organization of the disorganized molecules in an aggregate ordered structure to specifically function [38]. Weak non-covalent bonds such as hydrogen bonds, ionic bonds, electrostatic attractions, van der Waals interactions and hydrophobic interactions help to maintain the self-assembled molecule structures [39]. However, if these weak interactions are combined and act together, they create very stable supra-molecular assemblies. Peptides and proteins are self-assembled molecules which form discrete secondary and tertiary nanofibrous functional structures [40]. Hydrogen bonding in the polypeptide chains with a primary structure containing different amino acids create secondary structures such as alpha helices and beta sheets. Figure 2.3. represents the schematic of this self-assembly process. The advantage of the self-assembly technique over other fabrication techniques is producing much smaller nanofibers. Though, limited porous structure and low mechanical strength of self-assembled peptides are the main drawbacks of this fabrication technique.

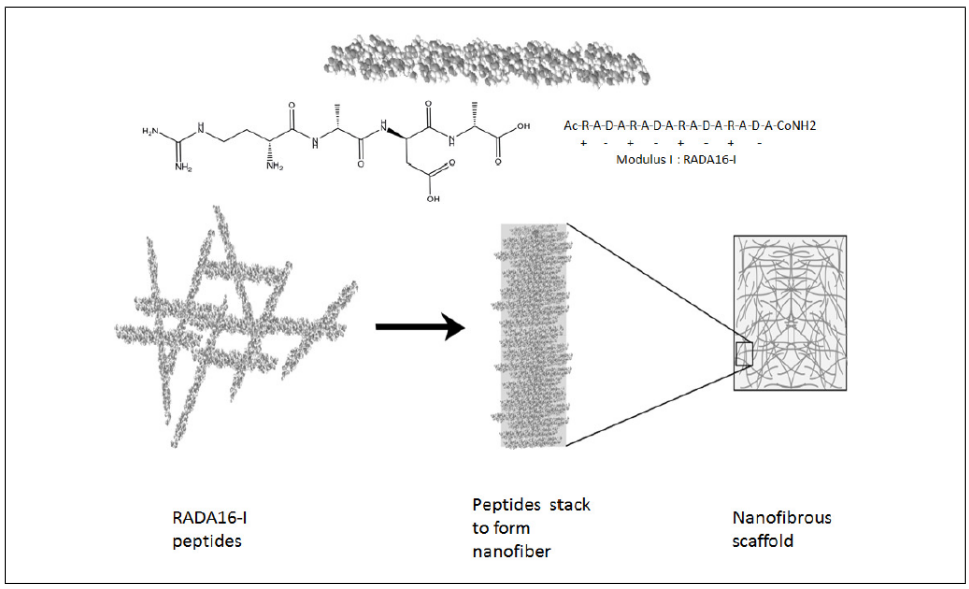

Figure 2.3 Molecular model of RADA16 self-assembling peptide [41].

In the electrospinning technique, the electrostatic force provides the fabrication of polymeric nanofibers ranging from nanoscale to microscale. High voltage creates electrostatic field to charge polymer solution droplet surface and eject a liquid jet

through a collector. When the applied electric field becomes higher than the surface tension of the polymer solution, which is held in the syringe, the polymer solution is ejected through the collector (Figure 2.4). Before the electrospun nanofibers are collected on the grounded collector, the solvent in the polymer solution evaporates [28, 30, 42, 43]. System parameters such as polymer molecular weight and distribution affect the rate of nanofiber degradation. The nanofiber diameter changes depending on polymer solution properties such as surface tension, conductivity, and viscosity. Process parameters such as, electric potential and flow rate of polymer, also have significant effect on fiber diameter. Electrospinning has been widely used to fabricate NF from natural and synthetic polymers to fabricate scaffolds and electrospun NF properties can be easily tuned to mimic the natural structure of a bone with desired physical properties such as high porous and a large surface area which might subsequently enhance cellular behaviours such as cell adhesion, proliferation, and differentiation [44] - [47]. High surface to volume ratio is a typical characteristic of NFs and plays an important role in providing bone-tissue mimetic morphology to enhance both cell-scaffold interaction and bone regeneration [44] - [47].

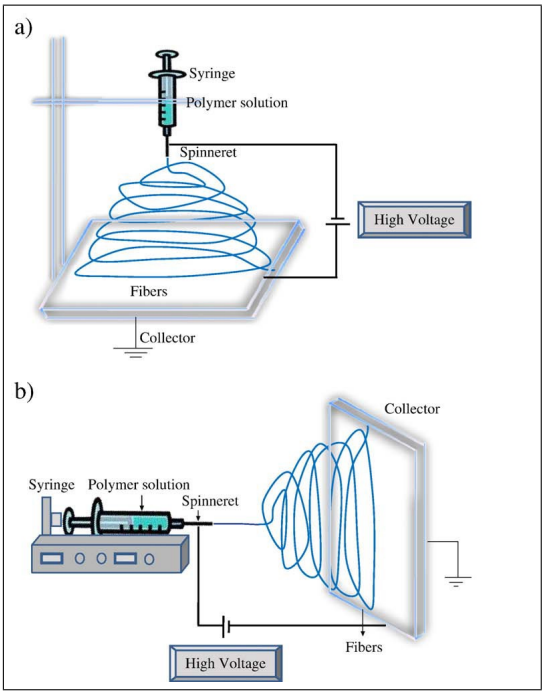

Figure 2.4 Electrospinning device set up (a) vertical set up and (b) horizontal set up of electrospinning devices [48].

2.5 Surface Modification Techniques

Surface treatment is used for modification of outer layer of polymers by introducing functional groups on the surface to increase its adhesion to other materials, wettability, resistance to coating, or biological environment interaction, while sustaining the desired properties [49]. Chemical and physical methods have been used to modify the polymer surface in biomaterial applications. The main focus of polymer surface modification are biocompatibility, specific protein and bio-inspired molecule interactions. Although chemical methods have been used for modification of polymeric material surfaces for years, physical surface treatment methods have been improved to produce oxygen containing functional groups on the surface in order to enhance wettability and adhesion to solve the chemical method related problems [50]. In chemical modification, the chemical agents can cause environmental problems and undesired changes in the polymer integrity. Suitable coating should provide substrate attachment and appropriate mechanical and functional properties. Some of the most common physical methods, such as corona and flame discharge, plasma based and radiation-induced treatments recently used to overcome chemical polymer modification related problems and provide suitable polymer coatings [49, 50].

Plasma is composed of free electrons, free radicals, electrically excited species, reactive oxygen and nitrogen species and UV photons and defined as fourth matter of state. The average electron power in plasma varies from 1 to 10 eV, the electron density range between 10^9-10^{12} cm^3. In plasma, the ionization degree is as low as $1/10^6$ or as high as 0.3. Plasma formation occurs via ionization of the gas by exerting energy to the gas. The energy can be applied to the gas in the form of electrical energy to create plasma. When an external electrical field that is created under high voltage, is applied to the gas, first, applied electrical field accelerates free electrons. Accelerated electrons with gas atoms and molecules provide to remove electrons from gas molecules structures, causes electron avalanche and ionization of the gas. When the externally applied electric field speeds free electrons and free electrons get kinetic energy and their temperature might rise up to thousands of kelvins. Kinetic energy of free electrons is transferred to gas molecules during collisions in between free electrons and gas

molecules. Depending on the efficacy of the energy transfer from electrons to heavier ions and the neutral gas atoms and/or molecules, plasmas are classified as thermal (or hot or equilibrium) and non-thermal plasma (or cold or non-equilibrium). In cold plasmas, cooling of heavier ions and neutral gas atoms and/or molecules is more efficient than the energy transfer from electrons to them [51, 52]. Thus, the plasma remains in the room temperature and therefore, cold plasma could be applied heat sensitive biological substrates and biomaterials. Cold atmospheric plasma (CAP) treatment is an emerging technique and due to its applicability of on biological materials and biomaterials various applications of it including antimicrobial and anticancer activity, accelerated wound healing effect along with biomaterial modifications has been reported in the literature [53]. Reactive oxygen and nitrogen species (RONS) along with free radicals generated during formation of CAP could react with treated materials to obtain surface modification with no or minimal damage to surface [53]. Plasma-mediated surface modification is shown to improve cell attachment due to increase of hydrophilicity.

2.6 Designing of Biomimetic Fibrous Scaffolds

Current developments in regenerative medicine and bone tissue engineering have considerable improvements on artificial regeneration for tissue repair and transplantation [54] - [56]. Producing scaffolds, which are composed of natural or synthetic polymers with tunable properties and successfully mimic natural tissue, is one of the major targets in this field [57, 58]. Natural and synthetic polymers are being generally used in 3-D scaffolds for control of cell behaviour [57] - [60]. Biological recognition that highly supports cell function and adhesion can be considered as an advantage of natural polymers [61]. Nevertheless, they have disadvantages such as less control over their mechanical properties and biodegradability [29, 62]. Even though, unmodified synthetic polymers are commonly used scaffold materials in tissue engineering, one drawback of these scaffolds is absence of biological cues on the surface [63]. Biomimetic scaffolds made of synthetic biodegradable polymers cannot enhance cell attachment, proliferation, and differentiation as much as natural polymer due to lack of biological

recognition parts. Furthermore, unmodified polymeric scaffolds do little to engender biological activity, as most commercial polymers are biologically inert. There are several surface modification methods to associate biological function into nanofibrous materials [64]. Typically, these methods are based on chemical integration of cell directive peptides or growth factors into the scaffold [65]. The mechanical properties of the polymer should retain while biochemical signals ensuring activity following chemical modification [66].

Modification of a scaffold using bioactive molecules such as ECM proteins or peptides can activate desired signalling pathways and thus enhance functionality of scaffolds. Using peptides rather than native proteins have some advantages such as high resistance to pH or temperature changes, easier manipulation during grafting, low risk of pathogenic contamination/immune system triggering and chemical synthesis that provides precise control over the chemical composition of the peptide [67]. Peptides are used to modify the surface of the scaffold to provide biological ligands that can promote cell attachment, proliferation, differentiation and thus interaction between cells and scaffold. Materials that are modified with peptides have been shown to be more effective in bone formation. Recently, several groups have used bone ECM proteins mimetic peptides in surface modification of NF and demonstrated the positive impact of such modification on both cell adhesion and osteogenic differentiation [35, 68].

The mineralization process initiation in bone regeneration is regulated by ECM proteins such as osteocalcin, osteopontin and bone sialoprotein. These non-collagenous proteins contain largely aspartic acid (Asp) and glutamic acid (Glu) residues that are known as nucleation points for calcium phosphate (CaP) mineralization. There have been studies showing the individual effect of different repeating units of Asp and Glu sequences on mineralization and osteogenic differentiation [35, 69]. In a follow-up study, Barati *et al*. investigated the influence of supplementing the nucleation buffer with various organic acids on osteogenic differentiation of hMSCs seeded on glutamic acid functionalized NFs. CaP nucleation depended on the acidic strength and the number of hydroxyl groups capable of hydrogen bonding on organic acids. According to the results, citric acid showed the highest CaP nucleation and osteogenic extent of

differentiation [70] Ceylan et al. functionalized the surface of NFs with Glu-Glu-Glu (EEE) and demonstrated that this short peptide promoted a more mature osteogenic differentiation than Asp-Gly-Glu-Ala (DGEA), an osteoinductive collagen I derived peptide known to improve initial attachment, migration and osteogenic differentiation for hMSCs [71]. Oslzta *et al*. reported that poly-Asp sequences act as an analogue of non-collagenous acidic proteins when deposited on purified collagen NF which resulted in significantly improved mineralization [72]. However, to the best of our knowledge, a comparative study that evaluates the effect of repeating sequences of Asp and Glu on osteogenic differentiation of hMSCs when used to modify the surface of synthetic NF has not been reported.

In this study, first the performance of using CAP for conjugation of different non-collagenous ECM proteins mimetic peptides with PLGA electrospun NF was investigated and then, the influence of the ASP and GLU peptide sequences on bone regeneration was evaluated with respect to cytochemical, mRNA expression and immunofluorescence analysis. Electrospinning was used to fabricate FDA approved PLGA ultrafine NF. To promote the peptide-NF conjugation, CAP was adopted to introduce functional carboxyl (-COOH) groups on NF. The surface chemistry of the CAP treated and untreated NF was assessed using different techniques including Scanning Electron Microscopy (SEM), water contact angle measurements, and X-ray Photoelectron Spectroscopy (XPS). Since the composition of bone tissue ECM such as non-collageneous proteins play a major role in osteogenic differentiation and mineralization, modification of NF surface with biomimetic peptides resembling the functional units of these proteins may accelerate mineralization and osteogenic differentiation.

3. MATERIALS AND METHODS

3.1 Characterization of Peptide-Nanofiber Conjugation

3.1.1 Peptide Synthesis

All chemicals for peptide synthesis were purchased from AAPPTEC (Louisville, KY, USA). EEEEEE (Glu-Glu-Glu-Glu-Glu-Glu) and DDDDDD (Asp-Asp-Asp-Asp-Asp-Asp) peptide sequences, hereafter denoted by GLU and ASP respectively, were manually synthesized on 4-Methylbenzhydrylamine (MBHA) resin (0.67mmol/g loading capacity) by using 9-fluorenylmethoxycarbonyl (Fmoc) chemistry as previously described [35]. All amino acid couplings were performed with 2 equivalents (based on loading capacity of resin) of Fmoc-protected amino acid, O-Benzotriazole-N,N,N',N'-tetramethyluronium-hexafluoro-phosphate (HBTU; 2 equiv), hydroxybenzotriazole (HOBt; 2 equiv) and N, N-diisopropylethylamine (4equiv; DIEA) HBTU in N,N-Dimethylformamide (DMF) for 3 hours. 20% piperidine in DMF was added to resin for 30 minutes to remove Fmoc-protecting group. In all coupling and deprotection reaction, ninhydrin test was used were for monitoring. For the conjugation between fluorescein isothiocyanate (FITC) and the peptide, Fmoc protecting group of -Lys (EEEEEEK) was removed by using cleavage solution containing TFA (0,047 % (v/v)), triisopropylsilane (0.00125 % (v/v)), deionized water (0.00125 % (v/v)), and Dichloromethane (DCM) (0.95 % (v/v)). The resin was washed 6 times with 10ml of cleavage solution for 5 minutes followed by the DCM wash. Finally, the resins were washed with 5% (v/v) DIEA in DCM. The FITC coupling solution containing 389.40 mg (FITC; Sigma Aldrich, St. Louis, MO, USA) and 256.8 μl DIEA was prepared in 3.0 mL DMF and added on the reaction vessel covered with aluminium foil in order to prevent the photobleaching of FITC. Trifluoroacetic acid (TFA): triisopropylsilane (TIPS): H_2O solution at ratio of 95:2.5:2.5 was used to cleave resin from peptide. Evaporation of TFA was performed with the rotary evaporator. The peptide was washed with ice-cold diethyl ether three times and freeze-dried. Further, high-pressure liquid chromatogra-

phy (HPLC, Agilent 1260 Quaternary LC) equipped with mass spectrometry (Agilent 6530 Q-TOF) with an electrospray ionization (ESI) source was used to purify and characterize all peptides [35].

3.1.2 Fabrication and Characterization of Nanofibers

A 7.0 wt% PLGA was prepared from PLGA powder and 1,1,1,3,3,3-hexafluoro-2-propanol (HFIP; Matrix Scientific; Columbia) solvent with stirring. After the injection of the polymer solution into 5 ml syringe with 21-gauge needle, the syringe was placed to syringe pump. The positive electrode was connected to tip of the needle. The rotating wheel, powered by a direct current (DC) motor, was covered with aluminium and used as collector. The NFs were collected by glass coverslips in 13 mm diameter (VWR, Bristol, CT, USA) placed on collector. The NFs were produced with electrospinning which was conducted at 20 kV electrical potential, needle-to-collector distance of 15 cm, injection rate of 1.0 ml/h ,and rotation speed of 1200 rpm. After coating with gold (QUORUM; Q150 RES; East Sussex; United Kingdom), the NF were imaged with a Scanning Electron Microscope (SEM; Carl Zeiss Microscopy, Germany) at 3 kV accelerating voltage . The SEM software provide the scale bars in the images and the fiber diameters and distributions were calculated with IMAGEJ software (National Institutes of Health, Bethesda, MD, USA) for obtaining the average fiber diameter.

3.1.3 Peptide Conjugation of Nanofibers

CAP was applied on electrospun NF at 1.5 kHz frequency and 31kV of output voltage for 45 seconds at a fixed 1 mm of discharge gap. CAP treated NF and non-treated, hereafter denoted by pNF and NF, respectively, were thoroughly washed. 2-Morpholinoethanesulfonic acid buffer (MES; 0.1 M, pH 6.5) was prepared and the pH was adjusted with 0.1 NaOH. Using 0.1 MES buffer, EDC/ NHS solution (2 mM EDC and 5 mM NHS) was prepared and the solution was used for incubation of NFs for 40 minutes to create carboxyl-rich surfaces. Then, the NF was incubated in 1 mM ASP

and GLU peptide in sterile Phosphate Buffer Solution (PBS) in 4°C refrigerator for 24 hours. The NF was thoroughly rinsed with PBS before characterization.

The effect of CAP treatment for 15 s, 30 s, 45 s, 60 s, 90 s and peptide (ASP and GLU) conjugation on pNF and hydrophilicity of NF surface was evaluated by water contact angle measurements using KSV Attension Theta goniometer (Biolin Scientific, Stockholm, Sweden). Briefly, 10 μl deionized water was dropped to the nanofiber surface. The contact angle (θ) was measured after photographing the drop on the surface.

FTIR spectra of non-CAP treated NF, 45s CAP treated NF, non-CAP treated peptide conjugated NF (GLU-NF, ASP-NF), and 45s CAP treated peptide conjugated NF (GLU-pNF, ASP-pNF) were determined using a Nicolet iS5 spectrometer (Thermo Scientific, Madison, WI, USA) with 4 cm^{-1} of spectral resolution. The spectrometer with an iD5 attenuated total reflection (ATR) accessor which collects 16 scans in the 400-4000 cm^{-1} has a diamond crystal. Electrospun nanofibers were collected on the glass slides attached onto a rotating drum. Electrospinning time was fixed to 3 hours to obtain 1mm thick nanofiber mats. NFs were seperated from the glass slides. FTIR measurements were performed with three different samples of each group from three different points.

X-ray photoelectron spectroscopy (XPS) measurement was performed with non-CAP treated NF, 45 seconds CAP treated NF, non-CAP treated peptide conjugated NF, 45 seconds CAP treated peptide conjugated NF using a spectrometer (Thermo K-Alpha XPS, Thermo Fisher Scientific, West Palm Beach, FL, USA). The XPS data were recorded using monochromatic Al Kα excitation. An electron energy analyzer (180° double focussing) had a 128-multichannel detector system. The analysis chamber was allowed to pump with a pressure of 2x10^{-7} mbar. High-resolution spectra and survey spectra were obtained using a constant analyzer with 50 eV of pass energies for single-point analysis of the surface area of each sample. 45° of detector input angle and 300 μm of X-ray beam size were used. Data analysis and manipulation were performed using the Avantage XPS software with a Shirley/Smart type background

and Gaussian/Lorentzian peak shapes.

To determine peptide surface coverage on NF, fluorescein isothiocyanate (FITC) attached peptide was conjugated to NF. pNF, CAP treated FITC labelled GLU peptide conjugated NF (GLU-pNF), CAP treated FITC labelled ASP peptide conjugated NF (ASP-pNF) were imaged with an inverted fluorescent microscope (Olympus CKX41, Tokyo, Japan).

3.2 Osteogenic Differentiation of hMSCs on Nanofibers

3.2.1 Cell Seeding

Human bone marrow derived mesenchymal stem cells (hMSCs) (HMSC-AD-500, CLS cell lines Service, Lot#102, Eppelheim, Germany) was cultivated in basal medium (DMEM with 10% FBS, 100 units/mL penicillin, 100 μg/mL streptomycin). The medium was changed in every second days (d) and cells at passage 3 were used for seeding. The edges of 13 mm circular glass coverslip covered by the NF were coated by a silicone sealant (Dow Corning, MI) to avoid separation of the NF from coverslips. Ultraviolet (UV) radiation for 1 hour (h) was used to sterilization. After UV, NFs were rinsed with 70% ethanol for 30 min and washed three times with sterile PBS. NFs was conditioned in basal medium for 1 h and 50 μl MSC cell suspension (5x10^4 cells/cm^2) in basal medium was seeded on each sample. After the cells were incubated for 24 h, osteogenic medium (basal medium with 10 mM β-glycerophosphate, 100 nM dexamethasone, and 50 μg/mL ascorbic acid) was replaced with existing medium.For up to 28 d, the cells were cultured in a humidified 5% CO_2 incubator . The negative control group was determined as MSCs seeded on pNF and incubated in osteogenic medium.

For cell morphology observation on surface modified NF, actin filaments and cell nuclei were stained by phalloidin and DAPI, respectively as previously described (Merck Millipore, Actin Cytoskeleton and Focal Adhesion Staining Kit, Catalog No.

FAK100) [35]. Briefly, cell-seeded micro-sheets were rinsed twice with PBS and fixed with 4% paraformaldehyde (Sigma Aldrich, St. Louis, MO, USA) at 4°C for 20 minutes. Next, cells on NFs were permeabilized with 0.1% Triton X-100 in PBS for 5 minutes and blocked with 1.5% bovine serum albumin (BSA) in PBS for 30 minutes. Then, cell seeded NFs were incubated with Phalloidin in PBS for 1h at 4°C and DAPI for 5 minutes. The NF samples after staining were imaged with an inverted fluorescent microscope to observe cell morphology.

3.2.2 Osteogenic Differentiation of hMSCs on Nanofibers

At 7, 14, 21, and 28 days, NFs were rinsed with PBS and the lysates of samples were obtained by using 10 mM Tris with 0.2% triton in PBS. The sample lysates were used for determination of DNA content, ALPase activity and calcium content. DNA content, ALPase activity and calcium content of each groups were measured with DNA Quantification Kit (Sigma Aldrich, St. Louis, MO, USA), QuantiChrom ALPase assay (Bioassay Systems, Hayward, CA, USA) and QuantiChrom Calcium Assay (Bioassay Systems, Hayward, CA, USA), respectively [4].

Briefly, bisBenzimide H 33258 Solution were prepared and added on lysed samples in a 96-well plate. For measurement fluorescence (excited at a wavelength of 360 nm), a spectrophotometer (BioTek, Winooski, VT, USA) at an emission wavelength of 460 nm. Using ALP kit, ALP activity was evaluated by p-nitrophenylphosphate (pNPP) in alkaline solution at 405 nm. First, 50 μl of lysed sample to 200 mu total reaction volume were used to initiate the reaction by the addition of assay buffer, 5 mM magnesium acetate, and 10 mM pNPP in 96-well plate. Optical density (OD) in 405 nm was measured at initial time and after 4 minutes on multi plate reader (BioTek, Winooski, VT, USA). Calcium content of the NF was measured by adding 50 μl of the suspension to 150 μl of the working solution. After incubation, OD at 612 nm was correlated to the equivalent amount of Ca^{2+} using a calibration curve plotted with reference calcium solutions. Determination of total mineralization of each NF was obtained from calcium content which was measured. The measured ALP activities and

calcium contents were normalized to cell numbers by dividing to DNA contents at each time point.

3.2.3 Quantitative Real-Time PCR Analysis

At 7, 14, 21 and 28 d, Blood/Cell Total RNA Mini Kit (Geneaid, Sijhih City, Taiwan) was used to isolate total cellular RNA. Then,cDNA was converted from the extracted purified RNA by using M-MuLV First Strand cDNA Synthesis Kit (Biomatik, Ontario, Canada). The cDNA obtained was subjected to Step One Plus Real-time PCR system (Applied Biosystems, Foster City, USA) amplification with specific primers to related genes. Table 1 shows forward and reverse primers for RT-qPCR, including osteocalcin (OCN), osteopontin (OPN), Collagen type I (Col I) and glyceraldehyde 3-phosphate dehydrogenase (GAPDH) were purchased from Sentegen Biotechnology (Ankara, TURKEY) and used to evaluate gene expression [73, 74]. The gene differential expression of Osteopontin (OP), Osteocalcin (OC) and collagen type I (COL-1) was quantified by by StepOne Software v2.3 and Ct values were classified by 2(-$\Delta\Delta$Ct) method described elsewhere [35]. Every group was experimented in qPCR as doublet and repeated as triplicate (n = 6).

Table 3.1
Forward and reverse primers of Collagen Type I (Col-1), Osteopontin (OP), Osteocalcin (OC), and glyceraldehyde 3-phosphate dehydrogenase (GAPDH; housekeeping gene) (GAPDH) used to asses hMSCs differentiation in qRT-PCR amplification.

Genes	Forward Primer	Reverse Primer
Col-1	5'-TGACGAGAC CAAGAACTG-3'	5'-TCAGCCTTAGAC GCCTCAAT-3'
OP	5'-ATGAGATTGGCAGTGATT-3'	5'-TTC AAT CAG AAA CTG GAA-3'
OC	5'-TGTGAGCTCAATCCGGAC TGT-3'	5'-CCGATAGGCCTCCTGAAG C-3'
GAPDH	5'-AACAGCGACACCCACTCCTC-3'	5'-CATACCAGGAAATGAGCTTG-3'

3.2.4 Immunofluorescent Staining

For immunofluorescence staining, cell-seeded NFs were rinsed in PBS and 4% paraformaldehyde (Sigma Aldrich, St. Louis, MO, USA) was used for fixation at 4°C for 30 minutes. Next, NFs were immersed with 0.1% Triton X-100 in PBS for 1 hour and 1.5% Bovine Serum Albumin (BSA) in PBS was used for blocking with for 2 hours. Then, primary antibodies in PBS containing 1% BSA were added to samples and incubated 24 h at 4°C. Primary antibodies (Santa Cruz Biotechnology Inc., Santa Cruz, California, USA) were used included mouse monoclonal antibody against COL I (cat. no sc-59772; 1:50), mouse monoclonal against OP antibody (cat. no. sc-21742; 1:50), and mouse monoclonal antibody against OC (cat. no. sc-365797; 1:500). Fluorescence secondary antibodies (Santa Cruz Biotechnology Inc., Santa Cruz, California, USA) included m-IgG kappa BP-FITC (cat. no. sc-516140; 1:200) and m-IgG kappa BP-PE (cat. no. sc-21742; 1:200) were diluted with 1% BSA. The nuclei of cells and one of the antibodies for COL-I, OC, and OP were image after staining with 4,6-diamidino-2-phenylindole (DAPI, Sigma Aldrich, St. Louis, MO, USA). The expression pattern of COL-I, OP, and OC with light intensity and same exposure time were characterized via capturing images using an inverted fluorescence microscope (Olympus CKX41, Tokyo, Japan).

3.3 Statistical Analysis

All data are statistically analyzed by two-way ANOVA (SPSS 12.0, SPSS GmbH, Germany) and the Student-Newman-Keuls method as a post hoc test. p values at least less than 0.05. (*$p < 0.05$, **$p < 0.01$, ***$p < 0.001$) were used to determine significant differences between groups.

4. RESULTS and DISCUSSION

4.1 Characterization of GLU and ASP Conjugated Nanofibers

ASP and GLU peptides were conjugated on to the surface of CAP treated NF using EDC/NHS as coupling agents and further osteogenic differentiation of hMSCs were conducted on experimental groups of pNF (control), GLU-pNF, and ASP-pNF, as depicted in Figure 4.1. The amide reaction between amino and carboxyl groups is expected to be difficult as basic amino groups deprotonates carboxyl group forming a highly unreactive carboxylate. Usually some coupling reagents are used to activate the carboxyl group to improve the yield of a carboxylic acid/amine coupling. Due to simplicity and high efficiency, EDC/NHS are the most widely used coupling reagents. The reaction can also take place in aqueous solutions, which helps avoiding the toxic effects of organic solvents. Basically, EDC activates the carboxylic group on NFs, forming an unstable o-acylisourea intermediate in MES buffer, a suitable carbodiimide reaction buffer. Then, NHS replaces EDC, forming an NHS ester which is a more stable reactive than o-acylisourea intermediate and still susceptible to attack by the N of a primary amine, thus leading to an efficient conjugation at physiological pH. An SEM photomicrograph of PGLA NF produced by electrospinning is given in Figure 4.1 A_I. NF diameter distribution histogram was given in Figure 4.1 A_{II}. Diameter of the resulting NFs used throughout the study ranged from 100 to 400 nm and the mean diameter was calculated to be 246 $\pm$ 24 nm. Next, the impact of surface treatment with CAP on the morphology of NF was investigated. In summary, CAP was used to introduce carboxyl (-COOH) groups to the surface of NF for conjugation with bone ECM mimetic peptides. The surface of the NF was treated for 15, 30, 45, 60 and 90 seconds and the results were compared to non-CAP treated NF. As shown in Figure 4.1 B_{II-VI}, the morphology of the NF did not change drastically up to 45 s treatment. However, longer CAP treatment (60 and 90s) caused a significant change in the morphology of NF as they started to join together. Our results were consistent with Chen *et al.* who reported 40 s of CAP treatment did not change the morphology of

poly(L-lactic acid) (PLLA) NF and drastically increased carboxyl groups on NF surface [75]. Effect of plasma treatment on the nanofibers is mainly governed by oxidation process [47]. Moreover, various effects of plasma such as antimicrobial effect, increasing hydrophilicity on surfaces is treatment time dependent and increases with plasma treatment time [76][77]. Even though, further studies are needed and it is hard to draw a certain conclusion about the morphology change of nanofibers, extensive oxidation in consequence of increasing plasma treatment time is more likely responsible for the morphology change of nanofibers.

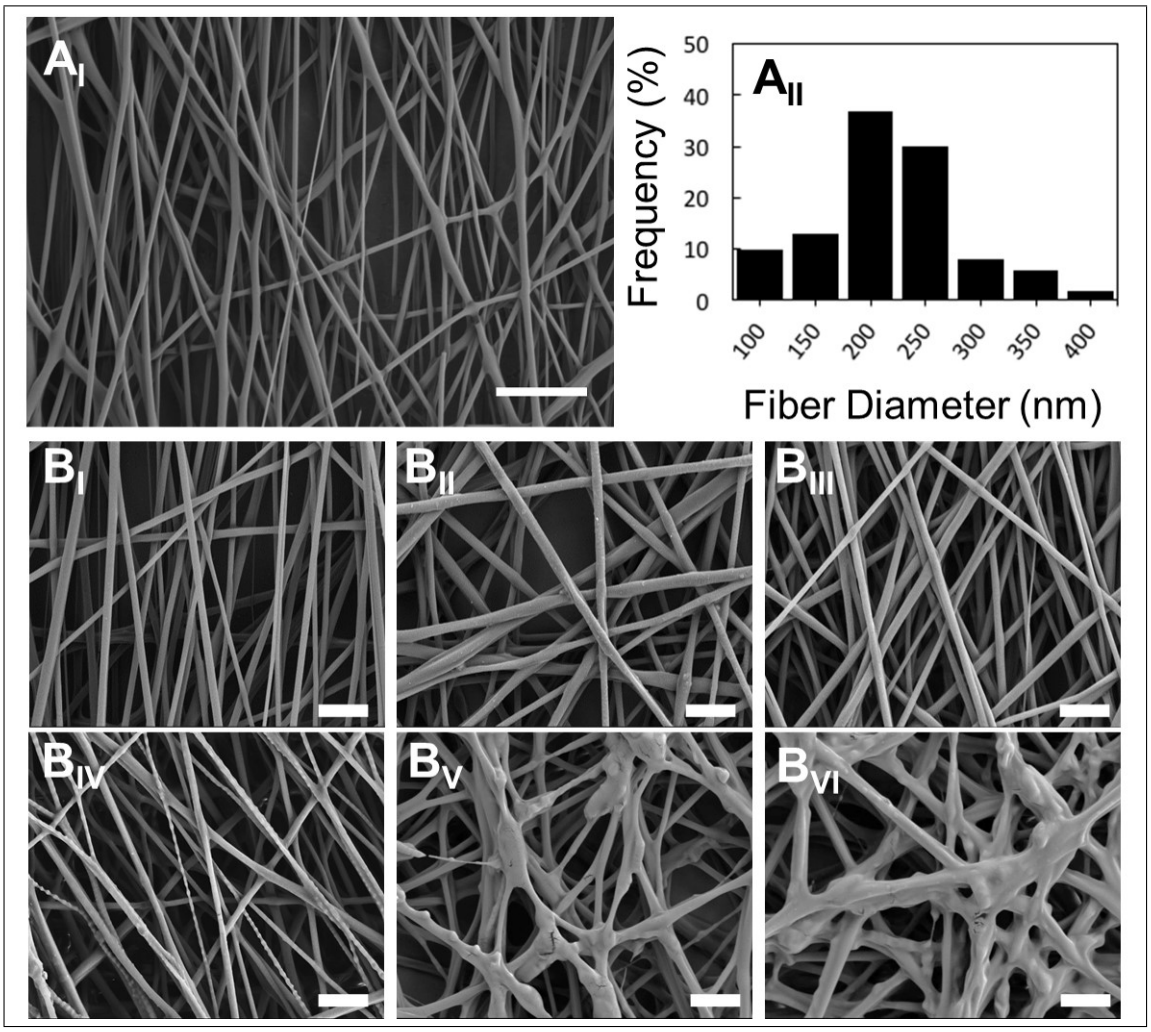

Figure 4.1 Scanning electron microscopy images of PLGA nanofibers (NF) (A_I) (Scale bar represents 200μm), histogram showing nanofiber diameters distribution (A_{II}), non-CAP treated (B_I), 15 (B_{II}), 30 (B_{III}), 45 (B_{IV}), 60 (B_V), and 90 (B_{VI}) seconds CAP treated PLGA NF (Scale bar represents 2μm).

The impact of CAP treatment for 15, 30, 45, 60 and 90 s on hydrophilicity of the NF was also demonstrated using water contact angle (θ) measurement. Water contact angle on NF were determined based on the images taken right after dripping 10 μL deionized water to the surface. They were compared to that of non-CAP treated NF. As demonstrated in Figure 4.1 B_{I-VI} that the contact angle (θ) of non-CAP treated NF was 124.83 ± 2.23° and dropped down to 36.72 ± 4.21° after 90 s CAP treatment. These results were in agreement with Dolci *et al.* who observed significant change on water contact angle and hydrophilicity of PLLA NF after CAP treatment, due to the increased carboxyl groups (-COOH) [78]. Effects of cold plasma treatment on nanofibers are mainly governed by oxidation process. In the present study, air plasma was generated that is known to have oxidative effect due to presence of reactive oxygen species [47]. As shown and supported by FTIR and XPS analyses, plasma treatment cleaves C-C and C=C bonds on the backbone of the nanofiber, and ROS created in the plasma are bounded to free ends of the carbon atoms exposed by the cleavage of single and double bonds which consequently leads to formation of -COOH groups on the surface of nanofibers. To be able to enhance peptide conjugation, it is important to maximize and reproduce the introduction of -COOH groups to the NF without losing their integrity. For that purpose, 45 seconds was chosen as the optimum CAP treatment time duration in the following experiments. Accordingly, the impact of the GLU and ASP peptide conjugation on the water contact angle (θ) of non-CAP treated (GLU-NF and ASP-NF) and 45 s CAP treated NF (GLU-pNF and ASP-pNF) were also shown (Figure 4.1 G-J). The water contact angles (θ) of GLU-NF (Figure 4.2 G), GLU-pNF (Figure 4.2 H), ASP-NF (Figure 4.2 I) and ASP-pNF (Figure 4.2 J) were measured as 62.46 ± 2.99°, 43.97 ± 1.49°, 60.79 ± 4.31° and 44.79 ± 1.31°, respectively. The water contact angles of GLU-NF and ASP-NF were measured to be lower than non-CAP treated NF (Figure 4.2 A), which is normal considering the fact that both GLU and ASP peptides are negatively charged at pH 7.0. The impact of CAP treatment on hydrophilicity of peptide modified scaffolds was evident in GLU-pNF and ASP-pNF because the water contact angle was considerably lower than that of non-CAP treated NF.

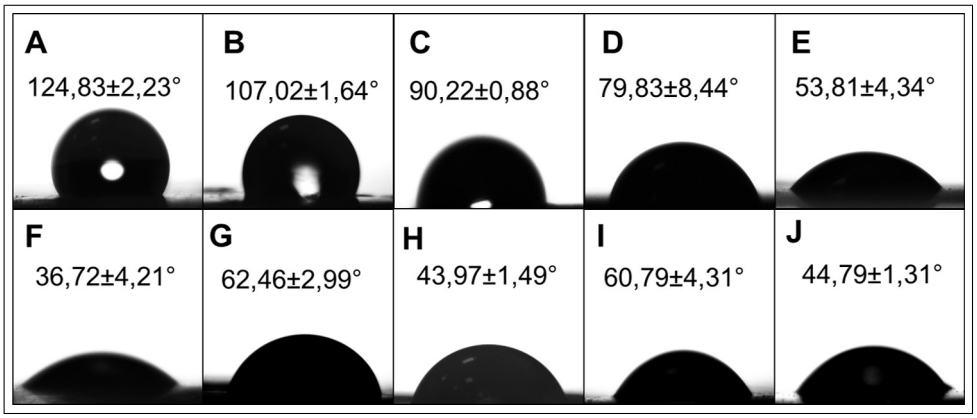

Figure 4.2 Water contact angles of surface modified nanofibers. Non-CAP treated (A), 15 s (B), 30 s (C), 45 s (D), 60 s (E) and 90 s CAP treated (F), non-CAP treated GLU peptide conjugated NF (GLU-NF) (G), 45 s CAP treated GLU peptide conjugated (GLU-pNF) (H), non-CAP treated ASP peptide conjugated (ASP-NF) (I) and 45 s CAP treated ASP peptide conjugated (ASP-pNF) (J).

ATR-FTIR spectroscopy was used to further confirm the surface group functionalization through CAP treatment. Figure 4.3 shows the FTIR spectra of the PLGA NF after CAP treatment (A_I) and/or peptide conjugation (A_{II-III}). In general, the broad bands at around 3600 and 3000 cm^{-1} are appeared due to the presence of hydroxyl and alkyl groups. The sharp bands around 1750 and 1080 cm^{-1} are assigned to the C=O stretch and the C-O stretch of the PLGA polymer [79, 80]. The bands occurring in the range of 1420-1400 cm^{-1} and 900-690 cm^{-1} are attributed to the CH_2, CH_2, and CH bending vibrations. The strong stretching bands due to the asymmetric and symmetric C-C(=O)-O vibrations are observed between 1200-1150 cm^{-1} [81]. There are also C-O-C bending bands appear in the 560-520 cm^{-1} region. In case of peptide conjugated NF, a change in the absorption bands at 3600-3000 cm^{-1} and 1460-1240 cm^{-1} was observed by the effect of nitrogen introduction due to the peptide conjugation. Compared to the spectra of non-treated (NF) and CAP treated (pNF) PLGA nanofibers, (Figure 4.3 A_I) the transmittance intensity of the PLGA NF was increased upon exposure to CAP treatment indicating the inclusion of oxygen-containing groups such as carbonyl and carboxyl, groups on the NF surface [82, 83]. The same trend was more predominantly observed for peptide conjugated (GLU-NF, ASP-NF) and CAP treated peptide conjugated (GLU-pNF, ASP-pNF) PLGA nanofibers (Figure 4A_{II-III}). Especially, the intensity of C-C(=O)-O, C-O, and C-O-C bands of became large and the bands

broaden with CAP treatment. In addition, this functionalization shows the positive effect of CAP treatment on the peptide conjugation on the PLGA NF.

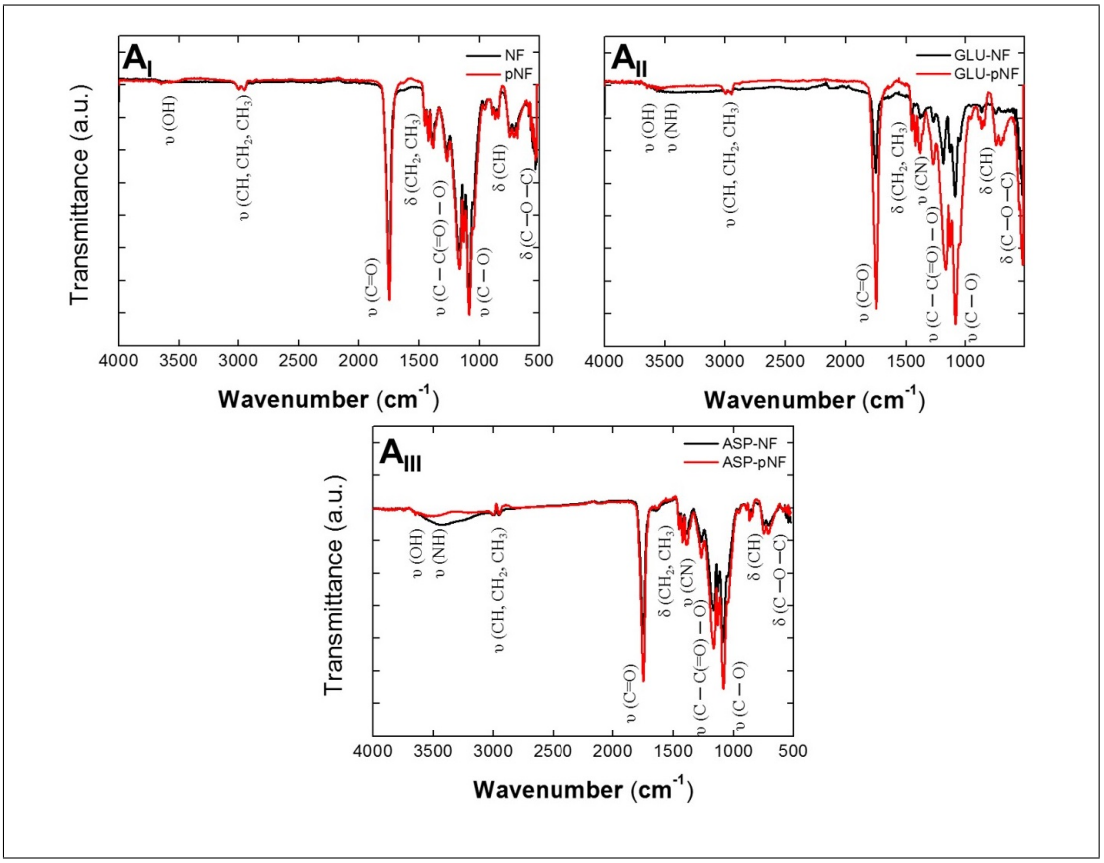

Figure 4.3 FTIR spectra for PLGA nanofibers (NF): before and after CAP treatment (NF and pNF) (A_I), GLU peptide conjugated (GLU-NF) and CAP treated GLU peptide conjugated (GLU-pNF) (A_{II}) ASP peptide conjugated (ASP-NF) and CAP treated ASP peptide conjugated (ASP-pNF) (A_{III}) (CAP treatment time is 45 seconds).

XPS analysis was also performed to investigate the changes in chemical composition of the PLGA nanofiber surfaces after CAP treatment and/or peptide conjugation. The elemental composition of the nanofiber surfaces was given in Table 2. Not surprisingly, the oxygen atomic concentration of the CAP treated NF is higher than that of the non-treated NF, indicating the formation of oxygen-rich functional groups with CAP treatment. This observation also suggests that the enhanced surface modification of CAP treated NF by GLU and ASP peptides. Since the similarity in chemical structures of GLU and ASP, a slight difference in conjugation and/or CAP treatment was observed at peptide conjugated NF. Figure 4.4) shows XPS wide scan (A_I), N1s

(B_I, (B_{II})), and C1s high-resolution spectra (C_I, C_{II}, C_{III}, C_{IV}) of PLGA NF with different surface chemistries. The wide survey of the NF had peaks arising from the backbone of PLGA, namely carbon (284 eV) and oxygen (532 eV); and nitrogen (399 eV) that corresponded to GLU indicating the binding of the peptide on the NF surface. There are no N1s signals in NF and pNF, while N1s signals were observed for peptide conjugated and CAP treated peptide conjugated NF (GLU-NF, ASP-NF, GLU-pNF, and ASP-pNF). The enlarged N1s XPS spectra show the effect of CAP treatment on the peptide conjugation. N1s signals can be deconvoluted into the three components at approximately 401, 397, and 396 eV corresponding to N-O, N=C, and N-C bonds [82]. C1s high-resolution XPS spectra showed main signals observed at 289, 287, 285, and 284 eV which arise from three carbon environments, which were O=C-O, C-O, C-(C,H), respectively [84]. GLU and ASP both have the same carbon environments [85]. CAP treatment changes these atomic compositions, especially, the intensity of O=C-O and C-O bonds significantly increased compared to that of non-treated PLGA nanofibers (NF). XPS analysis proved that the number of polar groups on PLGA NF surface increased after plasma treatment and the enhanced surface hydrophilicity enables peptide conjugation. This result seems to be in line with the FTIR measurements.

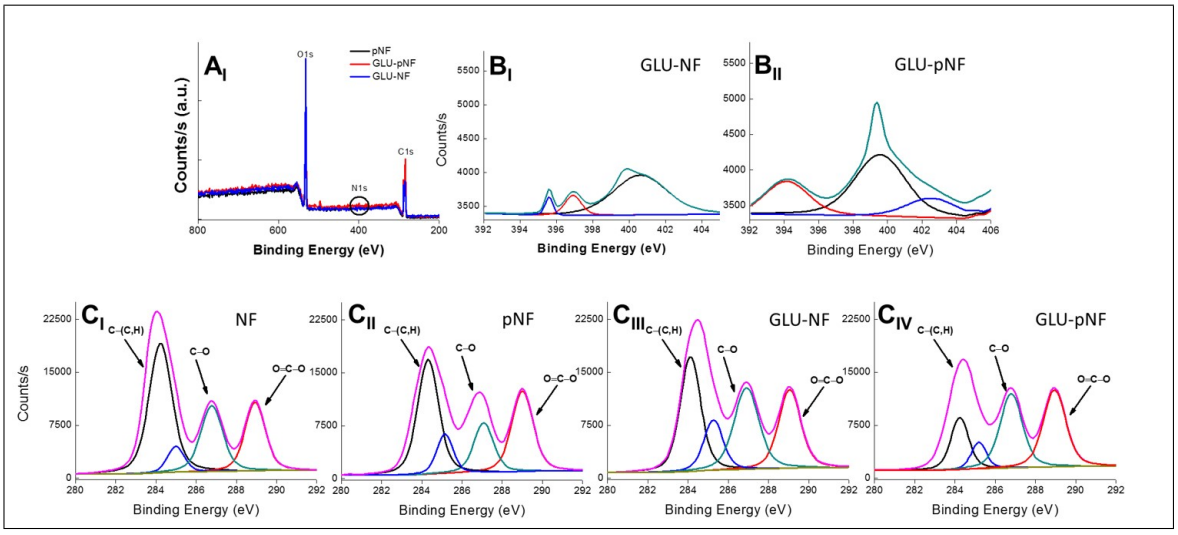

Figure 4.4 XPS wide scan (A_I) of CAP treated NF (pNF), non-CAP treated GLU peptide conjugated NF (GLU-NF), and CAP treated GLU peptide conjugated NF (GLU-pNF). N1s high-resolution spectra (B_I,B_{II}) of the GLU-NF and GLU-pNF. C1s high-resolution spectra (C_I, C_{II},C_{III},C_{IV}) of NF, pNF, GLU-NF, and GLU-pNF. (CAP treatment time is 45 seconds).

The efficacy of CAP treatment on peptide conjugation was also characterized via observing FITC intensity by using fluorescence microscope. FITC labeled GLU peptides were used to show the NF surface coverage with peptides. Briefly, FITC labelled GLU peptides were conjugated with the electrospun NF following 45 s CAP treatment. The images were then compared to those of NF, GLU-NF, and GLU-pNF. The mean (three different samples) fluorescence intensity of each image was also determined using IMAGEJ for further comparison. As shown in Figure 4.5A-B, the highest fluorescence intensity was observed with GLU-pNF. pNF only were used as negative control and as expected no fluorescence was observed, which confirms that the fluorescence observed in the other two images came from the label FITC. Karaman *et al.* indicated that CAP treatment on titanium discs increased the hydroxyl groups on the surface and that also sharply increased the FITC labelled RGD peptide conjugation [4]. Introduction of high number of carboxyl group to the surface with CAP, facilitated most of the surface to be covered with peptides. In addition, fluorescence intensity of GLU-pNF group showed significantly higher intensity compared to GLU-NF. It is speculated that available carboxyl groups even before CAP treatment facilitated peptide conjugation. Increasing carboxyl groups on NF surface via CAP treatment drastically increased peptide conjugation. Based on these findings, appropriate duration of CAP treatment could be used as an intermediate step to increase peptide conjugation to polymeric NF.

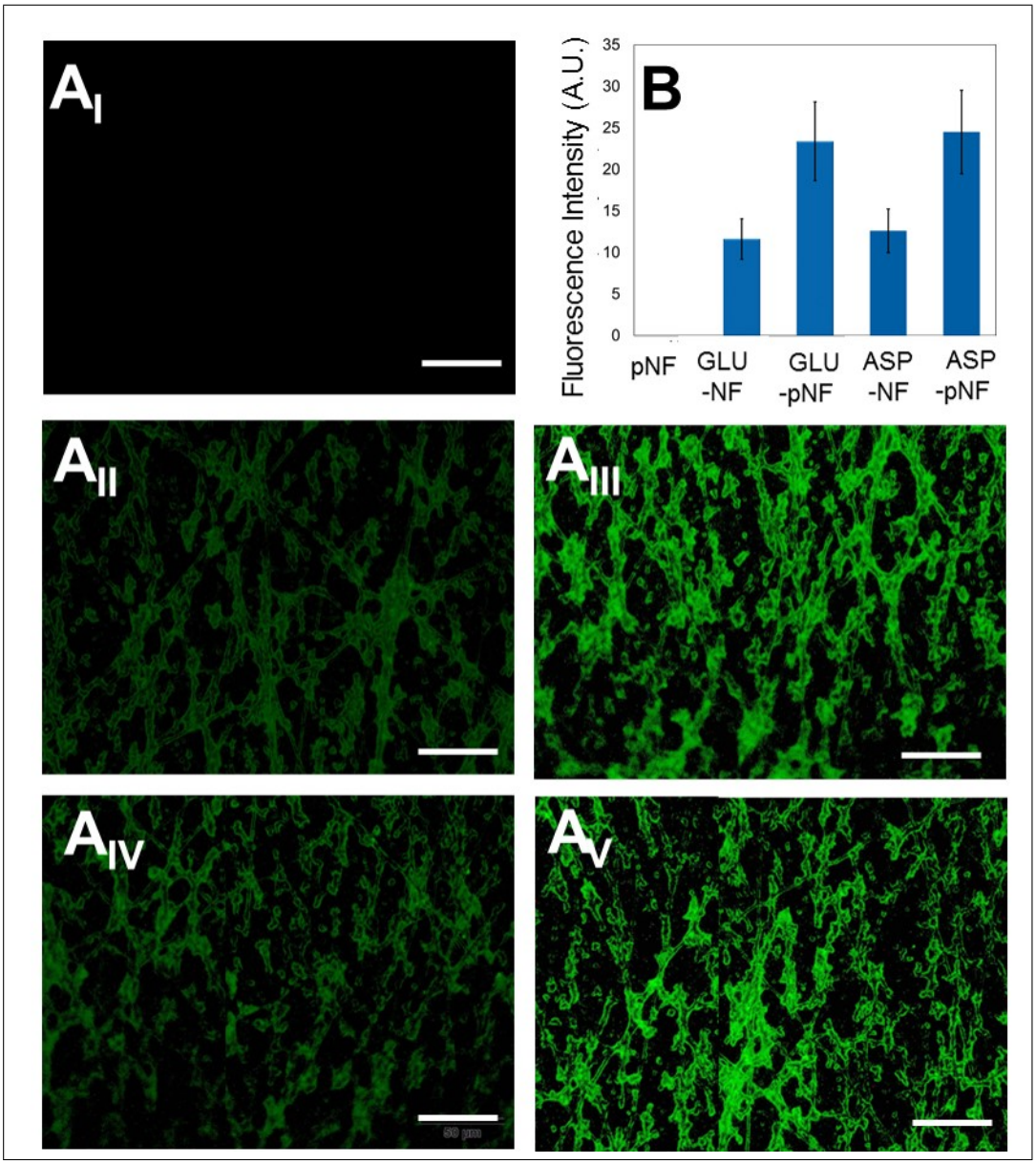

Figure 4.5 Fluorescent microscopy images of CAP treated pNF (A_I), non-CAP treated fluorescein isothiocyanate (FITC) labeled glutamic acid peptide conjugated NF (GLU-NF) (A_{II}), CAP treated FITC labeled glutamic acid peptide conjugated NF (GLU-pNF) (A_{III}), non-CAP treated fluorescein isothiocyanate (FITC) labeled aspartic acid peptide conjugated NF (ASP-NF) (A_{IV}), CAP treated FITC labeled aspartic acid peptide conjugated NF (ASP-pNF) ((A_V)) (Scale bar represents 50μm). Fluorescence intensity (A.U.) of pNF, GLU-NF, and GLU-pNF (B).

4.2 Differentiation of hMSCs on CAP treated GLU and ASP Conjugated NF

Osteogenic differentiation capability of hMSCs over pNF conjugated with GLU and ASP peptides was assessed, respectively. First the morphology of the cells on these surface modified NFs was examined after culturing in osteogenic medium for 7 days using a fluorescence microscopy. The actin cytoskeleton of cells was stained using phalloidin and nuclei with DAPI prior to fluorescence imaging. Resulting images show that hMSCs cells successfully attached and spread on pNF, GLU-pNF, and ASP-pNF (Figure 4.6). Additionally, it was previously reported that there is no difference in cell morphology of MSCs when seeded on neat PLGA NF, Glu enriched peptide conjugated NF and mineralized glutamic acid enriched peptide conjugated PLGA NF and cultured in osteogenic media [35]. Due to the fact that osteogenic media contains molecules that induce osteogenic differentiation, cell morphology on both groups resembles osteoblast.

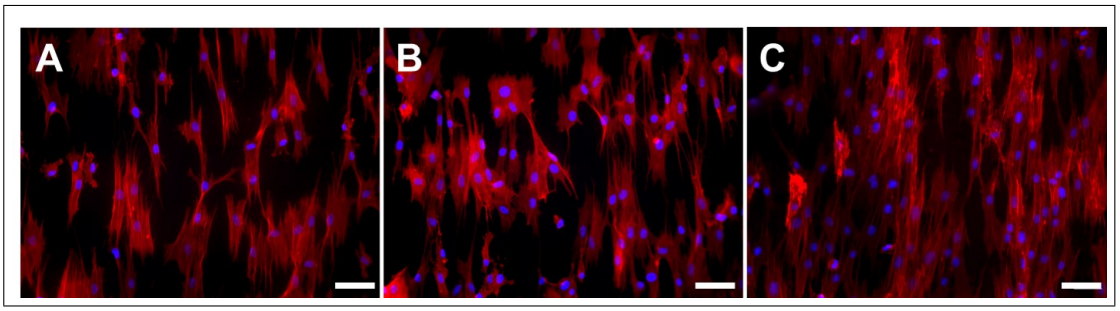

Figure 4.6 Morphology of human marrow stromal cells (hMSCs) seeded on CAP treated pNF (A), GLU-pNF (B), and ASP-pNF (C) after culturing in osteogenic media for 7 days. (Scale bar represents 50μm).

Differentiation of hMSCs into osteoblastic lineage is a complex process, which includes hMSCs adhesion, proliferation, differentiation, maturation, and mineralization [86]. Osteogenic differentiation can be guided through bone ECM mimetic peptide sequences and thus, bioinert synthetic scaffolds may gain transformed to osteoinductive capability [86]. The most crucial parameters that could be used to evaluate osteogenic differentiation are sufficient cell growth, ALP activity, calcium deposition and expression of osteogenic markers [86, 87, 88, 89]. In this regard, osteogenic differentiation of

hMSCs on surface modified NF was first quantified by monitoring cell number, ALP activity and calcium deposition over 28 d. The cell number was determined based on DNA content. At this stage, hMSCs were seeded and incubated on pNF, GLU-pNF, and ASP-pNF for 7, 14, 21 and 28 days and at the end of each culture time period, DNA content of cells were measured using a DNA quantification kit. Results revealed that ASP-pNF facilitated the proliferation of hMSCs significantly compared to GLU-pNF and pNF throughout the 28 days of incubation period (Figure 4.7A). This result suggest that ASP induces cell proliferation more than GLU, which can be related to the presence and more influential role of ASP in integrin binding motif [90]. As mentioned earlier, cell proliferation is the initial and key step for bone regeneration and directly coordinate the following maturation and mineralization stages [91]. Our results are consistent with early report that showed enhanced pre-osteoblasts proliferation when it was seeded on bone tissue ECM mimetic peptide conjugated synthetic scaffolds [92].

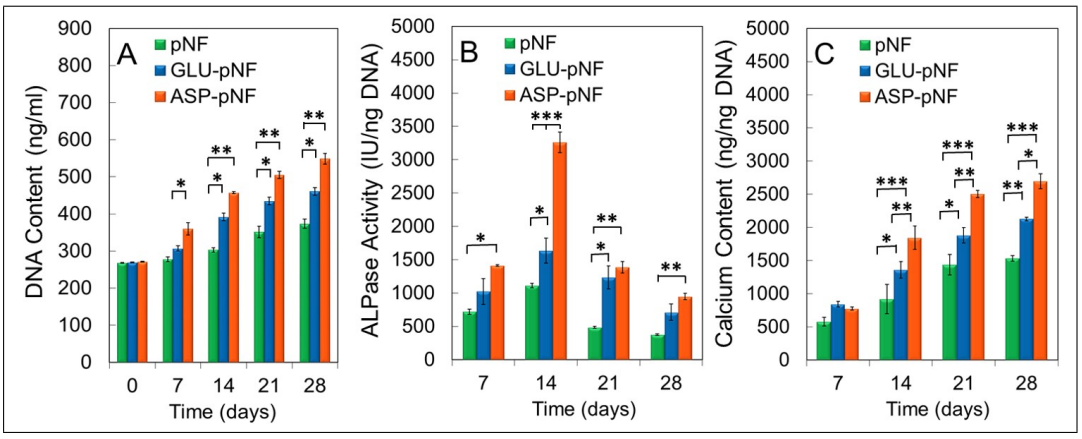

Figure 4.7 DNA content (A), ALP activity (B) and calcium content (C) of human marrow stromal cells (hMSCs) seeded on CAP treated pNF, GLU-pNF, and ASP-pNF in 28 days.

ALP activity measurement was carried out using the time-dependent pNPP formation in alkaline solution. As can be seen in Figure 4.7B, the ALP activity was the highest in the case of ASP-pNF at all time points when compared to other groups suggesting that cells did not receive as much osteogenic induction in pNF and GLU-pNF groups. Consistent with previous results, ALP activity appeared to rise from day 7 to 14, and then started to decrease with longer period of incubation with mineralization [35, 93, 94]. At day 14, ALP activity (IU/ng DNA) of ASP-pNF was

significantly higher (3261.9 ± 152.9) then those of pNF (1112.5 ± 33.4) and GLU-pNF (1636.8 ± 186.5). It should also be noted that ALP activity of cells on GLU-pNF was higher than those on pNF, indicating the positive impact of GLU on osteogenic differentiation. Calcium deposition is an indicative of maturation stage and for that hMSCs are expected to increase their calcium content [95]. hMSCs seeded groups of pNF, GLU-pNF, and ASP-pNF showed a consistent elevation of calcium content (ng Ca/ng DNA) throughout the incubation time and reached to 1531.8 ± 42.7 , 2127.1 ± 26.1, and 2695.5 ± 111.7, respectively. Results revealed that calcium content on ASP-pNF was significantly higher than pNF and GLU-pNF at all time points and peak at day 28 (Figure 4.7 C). Cells seeded on pNF only had the lowest calcium content, suggesting that cells did not mature as much compared to GLU-pNF and ASP-pNF. These results suggest that GLU and ASP conjugation sharply enhances mineralization of NF even at the early stages of culture and increased calcium phosphate content significantly accelerates osteogenic differentiation of hMSCs.In a recent study, Sun et al. indicated that seven ASP sequences implemented bone morphogenic protein (BMP) mimetic peptide [P28(D7)] significantly elevated ALP activity and Ca^{2+} content of MC3T3-E1 pre-osteoblasts. It was also demonstrated that ASP sequence had higher interaction with bone forming cells and minerals in osteogenic media compared to seven GLU sequence BMP mimetic peptide [P28(E7)] [96]. Additionally, they also reported that P28 peptide enriched nano-hydroxyapatite scaffolds significantly accelerated bone regeneration in critical-sized rat cranial defects at 6 and 12 weeks post-implantation compared with scaffolds lacking P28 [97].

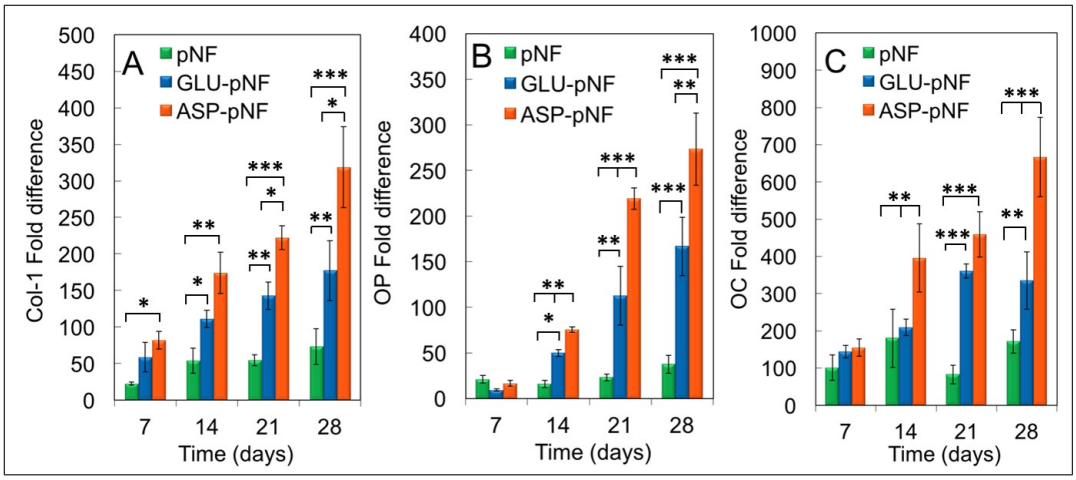

Figure 4.8 The mRNA expression fold difference of type 1 collagen (Col-I) (A), osteopontin (OP) (B), and osteocalcin (OC) (C) for hMSCs seeded on pNF, GLU-pNF, and ASP-pNF in 28 days.

Osteogenic differentiation was also evaluated with respect to expression of osteogenic markers including collagen type I (COL-I), osteopontin (OP) and osteocalcin (OC) using real-time PCR. Briefly, COL-I mineralizes in the presence of calcium ions into calcium phosphate which makes up roughly 70 % of bone matrix, whereas OPN and OCN are extracellular matrix proteins and they mediate nucleation and stabilization of calcium phosphate crystals [86, 95]. The expressions of all these markers are expected to rise throughout the 28 d of incubation considering their crucial role in bone crystallization. In line with the results obtained so far, ASP-pNF significantly induced expression of these markers as compared to pNF and GLU-pNF (Figure 4.8 A B C). The expression of all the markers on pNF only was the lowest, indicating the positive impact of the two peptides for bone mineralization. Importantly, it was indicated that negatively charged GLU and ASP peptides act as a calcium ion nucleation points in collagen NF during biomineralization and significantly increased the interaction of the NF with positively charged calcium ions [98]. Ca^{++} ions can bind to aminoacids with varying affinity depending on pH. Protonation of carboxylate group weakens the binding and thus, increasing the pH results in higher affinity. It has been previously reported that aspartate binds (Ka 7.0 $\pm$ 0.9 L / mol) Ca^{++} ions better than glutamate (Ka = 3.0 $\pm$ 0.8 L / mol) at a pH around 7 [99]. Therefore, it is possible that aspartate stabilizes CaP better than glutamate resulting in higher ALP activity, Ca content as

well as higher expression of osteogenic gene markers on NF at neutral pH [98]. Considering the inductive effect of mineralization on osteogenic differentiation, this might be one of the reasons for higher level osteogenic gene marker expression with ASP-pNF than Glu-pNF.

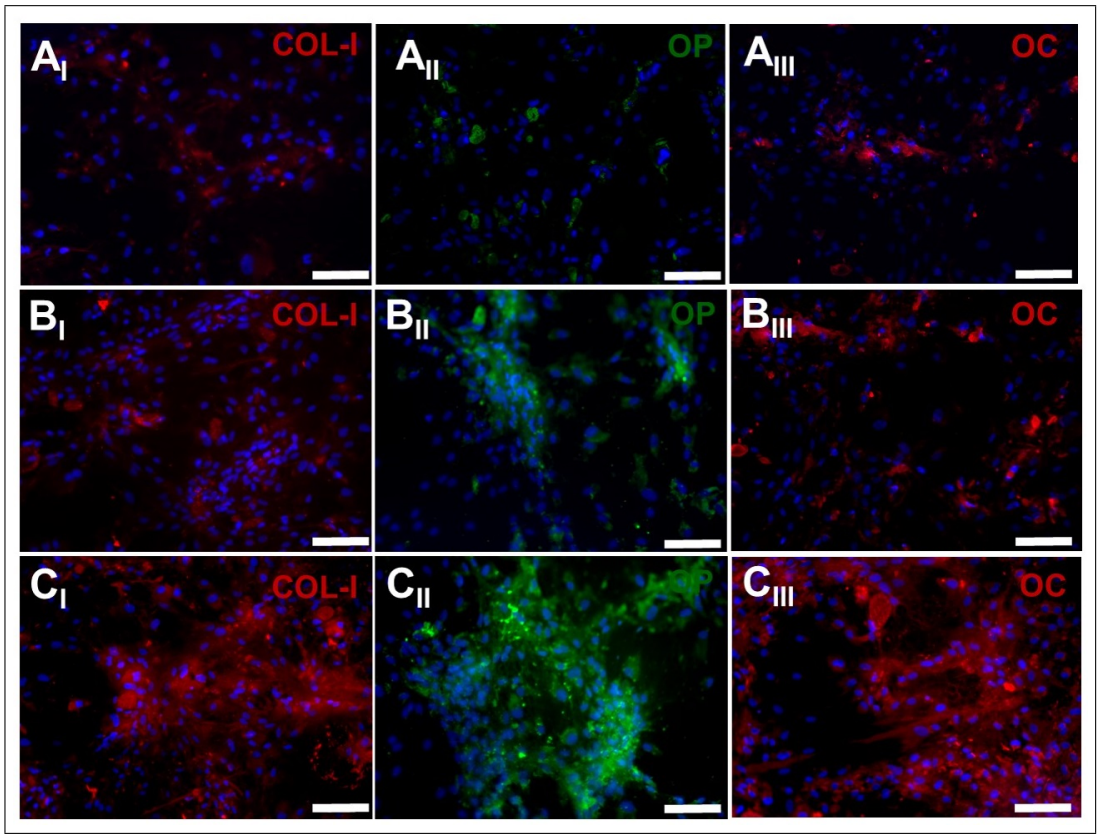

Figure 4.9 Expression of osteogenic markers type 1 collagen (A, red), osteopontin (OP) (B, green) and osteocalcin (OC) (C, red) for hMSCs seeded on CAP treated pNF (A_I, A_{II}, A_{III}), GLU-pNF (B_I, B_{II}, B_{III}), and ASP-pNF (C_I, C_{II}, C_{III}) after 28 days. (Scale bar represents 100μm).

Immunofluorescence staining of differentiated hMSCs also confirmed these results. Briefly, cells were incubated in osteogenic medium for 28 d and then chemically fixed for immunostaining. Lastly, proteins were stained using first primary antibodies against COL-I (red), OP (green) and OC (red) and then labelled with secondary antibodies to be visualized using an inverted fluorescence microscopy. As demonstrated in Figure 4.9, the expression of these osteogenic maturation related proteins was drastically higher for hMSCs on ASP-pNF than those on pNF and GLU-pNF, respectively. In consistent with real-time PCR results, cells on GLU conjugated NF showed an elevated

expression of these markers compared to those on pNF, highlighting the osteogenic inductive effect of GLU. In our previous study, we demonstrated that two GLU sequence including ECM mimetic peptide facilitated mineralization process and significantly increased gene expression and secretion of COL-I, OC, and OP [35]. Results so far have demonstrated that the presence of the two peptides (ASP and GLU) induced osteogenic significantly when compared to only CAP treatment. The two peptides seemed to show different osteogenic inductive effect with ASP being the highest.

5. CONCLUSIONS

In summary, biomimetic ASP and GLU templated peptides conjugated NF have been successfully fabricated via electrospinning. We found that application of CAP on the surface of NF increases hydrophilicity and carboxylic groups on PLGA NF surface, which could effectively enhance the binding sites for biomimetic GLU and ASP templated peptides. Conjugating GLU and ASP peptides improved the osteogenic differentiation ability of the NF. Moreover, ASP templated peptides sharply increased ALP activity, calcium content, and expression of key osteogenic markers of COL-1, OP, and OC compared to GLU conjugated and NF only. It was further depicted that ASP sequences are the major fragments that influence mineralization and osteogenic differentiation in non-collagenous proteins of bone extracellular matrix. Even though there are some studies showing the individual osteoinductive effect of ASP and GLU templated peptides when conjugated on synthetic scaffolds, there is no study in the literature that compares the osteoinductive effect of the two to the best of our knowledge. Our findings revealed that ASP templated peptides conjugated on PLGA NFs had more potential in inducing osteogenesis when used in peptides with the same number of repeats as GLU. There are a number of studies emphasizing the importance of enhancing the bioactivity of synthetic scaffolds for better bone tissue regeneration. It is believed that such findings will help researchers to design better biomimetic scaffolds to be translated into the clinic to improve bone healing processes.

REFERENCES

1. Seyedjafari, E., M. Soleimani, N. Ghaemi, and I. Shabani, "Nanohydroxyapatite-coated electrospun poly(l-lactide) nanofibers enhance osteogenic differentiation of stem cells and induce ectopic bone formation," *Biomacromolecules*, Vol. 11, no. 11, pp. 3118–3125, 2010.

2. Voss, P. J., A. Matsumoto, E. Alvarado, R. Schmelzeisen, F. Duttenhofer, and P. Poxleitner, "Treatment of stage ii medication-related osteonecrosis of the jaw with necrosectomy and autologous bone marrow mesenchymal stem cells," *Odontology*, Vol. 105, no. 4, pp. 484–493, 2017.

3. Peters, J., A. Robertson, C. Godavitarne, and B. Rogers, "Metabolic bone disease," *Orthopaedics and Trauma*, Vol. 31, no. 5, pp. 306–311, 2017.

4. Karaman, O., S. Kelebek, E. A. Demirci, F. Ibis, M. Ulu, and U. K. Ercan, "Synergistic effect of cold plasma treatment and rgd peptide coating on cell proliferation over titanium surfaces," *Tissue Engineering and Regenerative Medicine*, Vol. 15, no. 1, pp. 13–24, 2018.

5. Otto, S., C. Kleye, E. Burian, M. Ehrenfeld, and C.-P. Cornelius, "Custom-milled individual allogeneic bone grafts for alveolar cleft osteoplasty-a technical note," *Journal of Cranio-Maxillo-Facial Surgery*, Vol. 45, no. 12, pp. 1955–1961, 2017.

6. Chun, C., H. J. Lim, K. Y. Hong, K. H. Park, and S. C. Song, "The use of injectable, thermosensitive poly(organophosphazene)-rgd conjugates for the enhancement of mesenchymal stem cell osteogenic differentiation," *Biomaterials*, Vol. 30, no. 31, pp. 6295–308, 2009.

7. Hollinger, J., T. Einhorn, B. Doll, and C. Sfeir, *Bone Tissue Engineering*, Taylor Francis, 2004.

8. Kalfas, I. H., "Principles of bone healing," *Neurosurgical Focus*, Vol. 10, no. 4, pp. 1–4, 2001.

9. Marks, S. C., J., and S. N. Popoff, "Bone cell biology: the regulation of development, structure, and function in the skeleton," *The American Journal of Anatomy*, Vol. 183, no. 1, pp. 1–44, 1988.

10. Martini, F., J. Nath, E. Bartholomew, and R. Hutchings, *Fundamentals of Anatomy Physiology*, Pearson Education, Incorporated, 2017.

11. Rizzo, D., *Fundamentals of Anatomy and Physiology*, Cengage Learning, 2009.

12. Seeley, R., T. Stephens, and P. Tate, *Anatomy and Physiology*, McGraw-Hill Higher Education, 2003.

13. Buckwalter, J. A., and R. R. Cooper, "Bone structure and function," *Instructional Course Lectures American Academy of Orthopaedic Surgeons*, Vol. 36, pp. 27–48, 1987.

14. Levi, B., B. Peault, and A. W. James, "Bone tissue engineering and regeneration," *BioMed Research International*, Vol. 2014, p. 137529, 2014.

15. Polo-Corrales, L., M. Latorre-Esteves, and J. E. Ramirez-Vick, "Scaffold design for bone regeneration," *Journal of Nanoscience and Nanotechnology*, Vol. 14, no. 1, pp. 15–56, 2014.

16. Amini, A. R., C. T. Laurencin, and S. P. Nukavarapu, "Bone tissue engineering: Recent advances and challenges," *Critical Reviews in Biomedical Engineering*, Vol. 40, no. 5, pp. 363–408, 2012.

17. Gong, T., J. Xie, J. Liao, T. Zhang, S. Lin, and Y. Lin, "Nanomaterials and bone regeneration," *Bone Research*, Vol. 3, p. 15029, 2015.

18. Williams, D. F., "There is no such thing as a biocompatible material," *Biomaterials*, Vol. 35, no. 38, pp. 10009–14, 2014.

19. Balagangadharan, K., S. Dhivya, and N. Selvamurugan, "Chitosan based nanofibers in bone tissue engineering," *International Journal of Biological Macromolecules*, Vol. 104, pp. 1372–1382, 2017.

20. Yaszemski, M., D. Trantolo, K. Lewandrowski, V. Hasirci, D. Altobelli, and D. Wise, *Tissue Engineering And Novel Delivery Systems*, CRC Press, 2003.

21. Ma, P. X., "Biomimetic materials for tissue engineering," *Advanced Drug Delivery Reviews*, Vol. 60, no. 2, pp. 184–198, 2008.

22. Ulery, B. D., L. S. Nair, and C. T. Laurencin, "Biomedical applications of biodegradable polymers," *Journal of Polymer Science. Part B, Polymer Physics*, Vol. 49, no. 12, pp. 832–864, 2011.

23. Kim, M. S., J. H. Kim, B. H. Min, H. J. Chun, D. K. Han, and H. B. Lee, "Polymeric scaffolds for regenerative medicine," *Polymer Reviews*, Vol. 51, no. 1, pp. 23–52, 2011.

24. Cen, L., W. Liu, L. Cui, W. Zhang, and Y. Cao, "Collagen tissue engineering: development of novel biomaterials and applications," *The Journal of Pediatric Research*, Vol. 63, no. 5, pp. 492–6, 2008.

25. Lee, C. H., A. Singla, and Y. Lee, "Biomedical applications of collagen," *International Journal of Pharmaceutics*, Vol. 221, no. 1-2, pp. 1–22, 2001.

26. Malafaya, P. B., G. A. Silva, and R. L. Reis, "Natural-origin polymers as carriers and scaffolds for biomolecules and cell delivery in tissue engineering applications," *Advanced Drug Delivery*, Vol. 59, no. 4-5, pp. 207–33, 2007.

27. Chen, Z., Y. Song, J. Zhang, W. Liu, J. Cui, H. Li, and F. Chen, "Laminated electrospun nha/phb-composite scaffolds mimicking bone extracellular matrix for bone tissue engineering," *Materials Science and Engineering: C*, Vol. 72, pp. 341–351, 2017.

28. Vasita, R., and D. S. Katti, "Structural and functional characterization of proteins adsorbed on hydrophilized polylactide-co-glycolide microfibers," *International Journal of Nanomedicine*, Vol. 7, pp. 61–71, 2012.

29. Zhang, H., X. Mao, D. Zhao, W. Jiang, Z. Du, Q. Li, C. Jiang, and D. Han, "Three dimensional printed polylactic acid-hydroxyapatite composite scaffolds for prefabricating vascularized tissue engineered bone: An in vivo bioreactor model," *Scientific Reports*, Vol. 7, no. 1, p. 15255, 2017.

30. Katta, P., M. Alessandro, R. D. Ramsier, and G. G. Chase, "Continuous electrospinning of aligned polymer nanofibers onto a wire drum collector," *Nano Letters*, Vol. 4, no. 11, pp. 2215–2218, 2004.

31. Tran, R. T., W. M. Choy, H. Cao, I. Qattan, J.-C. Chiao, W. Y. Ip, K. W. K. Yeung, and J. Yang, "Fabrication and characterization of biomimetic multichanneled crosslinked-urethane doped polyester (cupe) tissue engineered nerve guides," *Journal of Biomedical Materials Research. Part A*, Vol. 102, no. 8, pp. 2793–2804, 2014.

32. Gao, X., J. Song, Y. Zhang, X. Xu, S. Zhang, P. Ji, and S. Wei, "Bioinspired design of polycaprolactone composite nanofibers as artificial bone extracellular matrix for bone regeneration application," *ACS Applied Materials and Interfaces*, Vol. 8, no. 41, pp. 27594–27610, 2016.

33. Hong, Y., R. L. Legge, S. Zhang, and P. Chen, "Effect of amino acid sequence and ph on nanofiber formation of self-assembling peptides eak16-II and eak16-IV," *Biomacromolecules*, Vol. 4, no. 5, pp. 1433–42, 2003.

34. Abouzari-lotf, E., H. Ghassemi, M. M. Nasef, A. Ahmad, M. Zakeri, T. M. Ting, A. Abbasi, and S. Mehdipour-Ataei, "Phase separated nanofibrous anion exchange membranes with polycationic side chains," *Journal of Materials Chemistry A*, Vol. 5, no. 29, pp. 15326–15341, 2017.

35. Karaman, O., S. Kelebek, E. A. Demirci, F. Ibis, M. Ulu, and U. K. Ercan, "Synergistic effect of cold plasma treatment and rgd peptide coating on cell proliferation over titanium surfaces," *Tissue Engineering and Regenerative Medicine*, Vol. 15, no. 1, pp. 13–24, 2018.

36. Keane, T. J., and S. F. Badylak, "Biomaterials for tissue engineering applications," *Seminars in Pediatric Surgery*, Vol. 23, no. 3, pp. 112–8, 2014.

37. Zhang, J. Y., E. J. Beckman, N. P. Piesco, and S. Agarwal, "A new peptide-based urethane polymer: synthesis, biodegradation, and potential to support cell growth in vitro," *Biomaterials*, Vol. 21, no. 12, pp. 1247–58, 2000.

38. Manasa, N., K. Priyadharshini, K. Uma Maheswari, and S. Swaminathan, "Self-assembling peptide nanofibrous scaffolds for tissue engineering: Novel approaches and strategies for effective functional regeneration," *Current Protein and Peptide Science*, Vol. 14, no. 1, pp. 70–84, 2013.

39. Kyle, S., A. Aggeli, E. Ingham, and M. J. McPherson, "Production of self-assembling biomaterials for tissue engineering," *Trends in Biotechnology*, Vol. 27, no. 7, pp. 423–433, 2009.

40. Silva, G. A., C. Czeisler, K. L. Niece, E. Beniash, D. A. Harrington, J. A. Kessler, and S. I. Stupp, "Selective differentiation of neural progenitor cells by high-epitope density nanofibers," *Science*, Vol. 303, no. 5662, pp. 1352–5, 2004.

41. Nune, D. M., P. Kumaraswamy, U. Maheswari Krishnan, and S. Sethuraman, *Self-Assembling Peptide Nanofibrous Scaffolds for Tissue Engineering: Novel Approaches and Strategies for Effective Functional Regeneration*, Vol. 14, 2013.

42. Zhang, F., B. Zuo, Z. Fan, Z. Xie, Q. Lu, X. Zhang, and D. L. Kaplan, "Mechanisms and control of silk-based electrospinning," *Biomacromolecules*, Vol. 13, no. 3, pp. 798–804, 2012.

43. Li, W.-J., and R. S. Tuan, "Fabrication and application of nanofibrous scaffolds in tissue engineering," *Current Protocols in Cell Biology*, Vol. Chapter 25, pp. Unit–25.2, 2009.

44. Zheng, W., W. Zhang, and X. Jiang, "Biomimetic collagen nanofibrous materials for bone tissue engineering," *Advanced Engineering Materials*, Vol. 12, no. 9, 2010.

45. Stratton, S., N. B. Shelke, K. Hoshino, S. Rudraiah, and S. G. Kumbar, "Bioactive polymeric scaffolds for tissue engineering," *Bioactive Materials*, Vol. 1, no. 2, pp. 93–108, 2016.

46. Jun, I., H.-S. Han, J. R. Edwards, and H. Jeon, "Electrospun fibrous scaffolds for tissue engineering: Viewpoints on architecture and fabrication," *International Journal of Molecular Sciences*, Vol. 19, no. 3, p. 745, 2018.

47. Karaman, O., M. Sen, and E. Demirci, "Electrospun scaffolds for vascular tissue engineering," in *Electrospun Materials for Tissue Engineering and Biomedical Applications*, pp. 261–287, Elsevier, 2017.

48. Bhardwaj, N., and S. C. Kundu, "Electrospinning: A fascinating fiber fabrication technique," *Biotechnology Advances*, Vol. 28, no. 3, pp. 325–347, 2010.

49. Huang, F., Q. Wei, and Y. Cai, "6 - surface functionalization of polymer nanofibers," in *Functional Nanofibers and their Applications* (Wei, Q., ed.), pp. 92–118, Woodhead Publishing, 2012.

50. Said, H. M., N. G. Nik Salleh, M. S. Alias, and A. W. M. El-Naggar, "Synthesis and characterization of hard materials based on radiation cured bio-polymer and nanoparticles," *Journal of Radiation Research and Applied Sciences*, Vol. 6, no. 2, pp. 71–78, 2013.

51. Fridman, G., G. Friedman, A. Gutsol, A. B. Shekhter, V. N. Vasilets, and A. Fridman, "Applied plasma medicine," *Plasma Processes and Polymers*, Vol. 5, no. 6, pp. 503–533, 2008.

52. Alkawareek, M. Y., S. P. Gorman, W. G. Graham, and B. F. Gilmore, "Potential cellular targets and antibacterial efficacy of atmospheric pressure non-thermal plasma," *International Journal of Antimicrobial Agents*, Vol. 43, no. 2, pp. 154–160, 2014.

53. Pizzi, A., and K. L. Mittal, *Handbook of Adhesive Technology*, CRC Press, 2017.

54. Wu, T., J. Zhang, Y. Wang, D. Li, B. Sun, H. El-Hamshary, M. Yin, and X. Mo, "Fabrication and preliminary study of a biomimetic tri-layer tubular graft based on fibers and fiber yarns for vascular tissue engineering," *Materials Science and Engineering: C*, Vol. 82, no. Supplement C, pp. 121–129, 2018.

55. Silva, A. M., J. H. Teixeira, M. I. Almeida, R. M. Goncalves, M. A. Barbosa, and S. G. Santos, "Extracellular vesicles: Immunomodulatory messengers in the context of tissue repair/regeneration," *European Journal of Pharmaceutical Sciences*, Vol. 98, no. Supplement C, pp. 86–95, 2017.

56. Pan, M., X. Wang, Y. Chen, S. Cao, J. Wen, G. Wu, Y. Li, L. Li, C. Qian, Z. Qin, Z. Li, D. Tan, Z. Fan, W. Wu, and J. Guo, "Tissue engineering with peripheral blood-derived mesenchymal stem cells promotes the regeneration of injured peripheral nerves," *Experimental Neurology*, Vol. 292, no. Supplement C, pp. 92–101, 2017.

57. Xu, Y., D. Xia, J. Han, S. Yuan, H. Lin, and C. Zhao, "Design and fabrication of porous chitosan scaffolds with tunable structures and mechanical properties," *Carbohydrate Polymers*, Vol. 177, no. Supplement C, pp. 210–216, 2017.

58. Lu, G., S. Liu, S. Lin, D. L. Kaplan, and Q. Lu, "Silk porous scaffolds with nanofibrous microstructures and tunable properties," *Colloids and Surfaces B: Biointerfaces*, Vol. 120, no. Supplement C, pp. 28–37, 2014.

59. Gutierrez-Hernandez, J. M., D. M. Escobar-Garcia, A. Escalante, H. Flores, F. J. Gonzalez, P. Gatenholm, and G. Toriz, "In vitro evaluation of osteoblastic cells on bacterial cellulose modified with multi-walled carbon nanotubes as scaffold for bone regeneration," *Materials Science and Engineering: C*, Vol. 75, no. Supplement C, pp. 445–453, 2017.

60. Zhao, X., L. Zhou, Q. Li, Q. Zou, and C. Du, "Biomimetic mineralization of carboxymethyl chitosan nanofibers with improved osteogenic activity in vitro and in vivo," *Carbohydrate Polymers*, Vol. 195, pp. 225–234, September 2018.

61. Maiti, S., S. Jana, and S. Jana, "1 - biocomposites in therapeutic application: Current status and future," in *Biopolymer-Based Composites* (Jana, S., S. Maiti, and S. Jana, eds.), pp. 1–29, Woodhead Publishing, 2017.

62. Abdellaoui, H., R. Bouhfid, and A. E. K. Qaiss, "Lignocellulosic fibres reinforced thermoset composites: Preparation, characterization, mechanical and rheological properties," in *Lignocellulosic Composite Materials* (Kalia, S., ed.), pp. 215–270, Cham: Springer International Publishing, 2018.

63. Xie, L., W. Qian, J. Sun, and B. Zou, "Engineering nanobiomaterials for improved tissue regeneration," *Nanobiomaterials: Classification, Fabrication and Biomedical Applications*, 2017.

64. Bas, O., D. D'Angella, J. G. Baldwin, N. J. Castro, F. M. Wunner, N. T. Saidy, S. Kollmannsberger, A. Reali, E. Rank, and E. M. De-Juan-Pardo, "An integrated design, material, and fabrication platform for engineering biomechanically and biologically functional soft tissues," *ACS Applied Materials Interfaces*, Vol. 9, no. 35, pp. 29430–29437, 2017.

65. Jordan, A. M., V. Viswanath, S.-E. Kim, J. K. Pokorski, and L. T. Korley, "Processing and surface modification of polymer nanofibers for biological scaffolds: a review," *Journal of Materials Chemistry B*, Vol. 4, no. 36, pp. 5958–5974, 2016.

66. Jordan, A. M., V. Viswanath, S.-E. Kim, J. K. Pokorski, and L. T. J. Korley, "Processing and surface modification of polymer nanofibers for biological scaffolds: a review," *Journal of Materials Chemistry B*, Vol. 4, no. 36, pp. 5958–5974, 2016.

67. Wang, C., Y. Liu, Y. Fan, and X. Li, "The use of bioactive peptides to modify materials for bone tissue repair," *Regenerative Biomaterials*, Vol. 4, no. 3, pp. 191–206, 2017.

68. Gao, X., X. Zhang, J. Song, X. Xu, A. Xu, M. Wang, B. Xie, E. Huang, F. Deng, and S. Wei, "Osteoinductive peptide-functionalized nanofibers with highly ordered structure as biomimetic scaffolds for bone tissue engineering," *International Journal of Nanomedicine*, Vol. 10, p. 7109, 2015.

69. Itoh, D., S. Yoneda, S. Kuroda, H. Kondo, A. Umezawa, K. Ohya, T. Ohyama, and S. Kasugai, "Enhancement of osteogenesis on hydroxyapatite surface coated with synthetic peptide (eeeeeeeprgdt) in vitro," *Journal of Biomedical Materials Research Part A*, Vol. 62, no. 2, pp. 292–298, 2002.

70. Barati, D., J. D. Walters, S. R. Pajoum Shariati, S. Moeinzadeh, and E. Jabbari, "Effect of organic acids on calcium phosphate nucleation and osteogenic differentiation of human mesenchymal stem cells on peptide functionalized nanofibers," *Langmuir*, Vol. 31, no. 18, pp. 5130–5140, 2015.

71. Ceylan, H., S. Kocabey, H. Unal Gulsuner, O. S. Balcik, M. O. Guler, and A. B. Tekinay, "Bone-like mineral nucleating peptide nanofibers induce differentiation of human mesenchymal stem cells into mature osteoblasts," *Biomacromolecules*, Vol. 15, no. 7, pp. 2407–2418, 2014.

72. Deshpande, A. S., and E. Beniash, "Bioinspired synthesis of mineralized collagen fibrils," *Crystal Growth and Design*, Vol. 8, no. 8, pp. 3084–3090, 2008.

73. Kang, Y., S. Kim, M. Fahrenholtz, A. Khademhosseini, and Y. Yang, "Osteogenic and angiogenic potentials of monocultured and co-cultured human-bone-marrow-derived mesenchymal stem cells and human-umbilical-vein endothelial cells on three-dimensional porous beta-tricalcium phosphate scaffold," *Acta Biomaterialia*, Vol. 9, no. 1, pp. 4906–4915, 2013.

74. Dang, C. V., K. A. O'Donnell, K. I. Zeller, T. Nguyen, R. C. Osthus, and F. Li, "The c-myc target gene network," *Seminars in Pediatric Surgery*, Vol. 16, no. 4, pp. 253–64, 2006.

75. Chen, J.-P., and C.-H. Su, "Surface modification of electrospun plla nanofibers by plasma treatment and cationized gelatin immobilization for cartilage tissue engineering," *Acta Biomaterialia*, Vol. 7, no. 1, pp. 234–243, 2011.

76. Ozan, K., "Mineralized nanofibers for bone tissue engineering," in *Advancing Medicine through Nanotechnology and Nanomechanics Applications* (Keka, T., B. Mayank, and M. Anil Shantappa, eds.), pp. 200–218, Hershey, PA, USA: IGI Global, 2017.

77. Fu, C., X. Yang, S. Tan, and L. Song, "Enhancing cell proliferation and osteogenic differentiation of mc3t3-e1 pre-osteoblasts by bmp-2 delivery in graphene oxide-incorporated plga/ha biodegradable microcarriers," *Scientific Reports*, Vol. 7, no. 1, p. 12549, 2017.

78. Dolci, L. S., S. D. Quiroga, M. Gherardi, R. Laurita, A. Liguori, P. Sanibondi, A. Fiorani, L. Calza, V. Colombo, and M. L. Focarete, "Carboxyl surface functionalization of poly (l-lactic acid) electrospun nanofibers through atmospheric non-thermal plasma affects fibroblast morphology," *Plasma Processes and Polymers*, Vol. 11, no. 3, pp. 203–213, 2014.

79. Jose, M. V., V. Thomas, D. R. Dean, and E. Nyairo, "Fabrication and characterization of aligned nanofibrous plga/collagen blends as bone tissue scaffolds," *Polymer*, Vol. 50, no. 15, pp. 3778–3785, 2009.

80. Meng, Z., Y. Wang, C. Ma, W. Zheng, L. Li, and Y. Zheng, "Electrospinning of plga/gelatin randomly-oriented and aligned nanofibers as potential scaffold in tissue engineering," *Materials Science and Engineering: C*, Vol. 30, no. 8, pp. 1204–1210, 2010.

81. Stevanovic, M. M., B. Jordovic, and D. P. Uskokovic, "Preparation and characterization of poly(d,l-lactide-co-glycolide) nanoparticles containing ascorbic acid," *Journal of Biomedicine Biotechnology*, no. 7, pp. 84965–84965, 2007.

82. Kim, H. J., I.-S. Bae, S.-J. Cho, J.-H. Boo, B.-C. Lee, J. Heo, I. Chung, and B. Hong, "Synthesis and characteristics of nh 2-functionalized polymer films to align and immobilize dna molecules," *Nanoscale Research Letters*, Vol. 7, no. 1, p. 30, 2012.

83. Mandracci, P., F. Mussano, P. Rivolo, and S. Carossa, "Surface treatments and functional coatings for biocompatibility improvement and bacterial adhesion reduction in dental implantology," *Coatings*, Vol. 6, no. 1, p. 7, 2016.

84. Dementjev, A., A. De Graaf, M. Van de Sanden, K. Maslakov, A. Naumkin, and A. Serov, "X-ray photoelectron spectroscopy reference data for identification of the c3n4 phase in carbon-nitrogen films," *Diamond and Related Materials*, Vol. 9, no. 11, pp. 1904–1907, 2000.

85. Stevens, J. S., A. C. de Luca, M. Pelendritis, G. Terenghi, S. Downes, and S. L. Schroeder, "Quantitative analysis of complex amino acids and rgd peptides by x-ray photoelectron spectroscopy (xps)," *Surface and Interface Analysis*, Vol. 45, no. 8, pp. 1238–1246, 2013.

86. Marie, P. J., and O. Fromigue, "Osteogenic differentiation of human marrow-derived mesenchymal stem cells," *Regenerative Medicine*, 2006.

87. Pina, S., J. M. Oliveira, and R. L. Reis, "Natural-based nanocomposites for bone tissue engineering and regenerative medicine: A review," *Advanced Materials*, Vol. 27, no. 7, pp. 1143–1169, 2015.

88. Kuo, Z.-K., P.-L. Lai, E. K.-W. Toh, C.-H. Weng, H.-W. Tseng, P.-Z. Chang, C.-C. Chen, and C.-M. Cheng, "Osteogenic differentiation of preosteoblasts on a hemostatic gelatin sponge," *Scientific Reports*, Vol. 6, p. 32884, 2016.

89. Barati, D., S. Moeinzadeh, O. Karaman, and E. Jabbari, "Time dependence of material properties of polyethylene glycol hydrogels chain extended with short hydroxy acid segments," *Polymer*, Vol. 55, no. 16, pp. 3894–3904, 2014.

90. Cherny, R., M. A. Honan, and P. Thiagarajan, "Site-directed mutagenesis of the arginine-glycine-aspartic acid in vitronectin abolishes cell adhesion," *Journal of Biological Chemistry*, Vol. 268, no. 13, pp. 9725–9729, 1993.

91. Lian, J. B., and G. S. Stein, "Concepts of osteoblast growth and differentiation: basis for modulation of bone cell development and tissue formation," *Critical Reviews in Oral Biology Medicine*, Vol. 3, no. 3, pp. 269–305, 1992.

92. Moore, N. M., N. J. Lin, N. D. Gallant, and M. L. Becker, "The use of immobilized osteogenic growth peptide on gradient substrates synthesized via click chemistry to enhance mc3t3-e1 osteoblast proliferation," *Biomaterials*, Vol. 31, no. 7, pp. 1604–1611, 2010.

93. He, X., J. Ma, and E. Jabbari, "Effect of grafting rgd and bmp-2 protein-derived peptides to a hydrogel substrate on osteogenic differentiation of marrow stromal cells," *Langmuir*, Vol. 24, no. 21, pp. 12508–12516, 2008.

94. Cha, C., W. B. Liechty, A. Khademhosseini, and N. A. Peppas, "Designing biomaterials to direct stem cell fate," *ACS Nano*, Vol. 6, no. 11, pp. 9353–9358, 2012.

95. Birmingham, E., G. L. Niebur, P. E. McHugh, G. Shaw, F. P. Barry, and L. M. McNamara, "Osteogenic differentiation of mesenchymal stem cells is regulated by osteocyte and osteoblast cells in a simplified bone niche," *European Cells and Material*, Vol. 23, pp. 13–27, 2012.

96. Sun, T., Y. Qu, W. Cui, L. Yang, Y. Ji, W. Yu, R. Navinduth, Z. Shao, H. Yang, and X. Guo, "Evaluation of osteogenic inductivity of a novel bmp2-mimicking peptide p28 and p28-containing bone composite," *Journal of Biomedical Materials Research Part A*, Vol. 106, no. 1, pp. 210–220, 2018.

97. Sun, T., K. Zhou, M. Liu, X. Guo, Y. Qu, W. Cui, Z. Shao, X. Zhang, and S. Xu, "Loading of bmp-2-related peptide onto three-dimensional nano-hydroxyapatite scaffolds accelerates mineralization in critical-sized cranial bone defects," *Journal of Tissue Engineering and Regenerative Medicine*, Vol. 12, no. 4, pp. 864–877, 2018.

98. Nudelman, F., A. J. Lausch, N. A. J. M. Sommerdijk, and E. D. Sone, "In vitro models of collagen biomineralization," *Journal of Structural Biology*, Vol. 183, pp. 258–269, August 2013.

99. Vavrusova, M., and L. H. Skibsted, "Calcium binding to dipeptides of aspartate and glutamate in comparison with orthophosphoserine," *Journal of Agricultural and Food Chemistry*, Vol. 61, no. 22, pp. 5380–4, 2013.